Published December 28, 2015

Cbx4 maintains the epithelial lineage identity and cell proliferation in the developing stratified epithelium

Andrei N. Mardaryev,[1] Bo Liu,[6] Valentina Rapisarda,[1] Krzysztof Poterlowicz,[1] Igor Malashchuk,[1] Jana Rudolf,[1] Andrey A. Sharov,[2] Colin A. Jahoda,[3] Michael Y. Fessing,[1] Salvador A. Benitah,[4,5] Guo-Liang Xu,[6] and Vladimir A. Botchkarev[1,2]

[1]Centre for Skin Sciences, School of Life Sciences, University of Bradford, Yorkshire BD7 1DP, England, UK
[2]Department of Dermatology, Boston University School of Medicine, Boston, MA 02118
[3]School of Biological Sciences, University of Durham, Durham DH1 3LE, England, UK
[4]Institute for Research in Biomedicine, 08028 Barcelona, Spain
[5]Catalan Institution for Research and Advanced Studies, 08010 Barcelona, Spain
[6]The State Key Laboratory of Molecular Biology, Institute of Biochemistry and Cell Biology, Chinese Academy of Sciences, Shanghai 200031, China

During development, multipotent progenitor cells establish lineage-specific programmers of gene activation and silencing underlying their differentiation into specialized cell types. We show that the Polycomb component Cbx4 serves as a critical determinant that maintains the epithelial identity in the developing epidermis by repressing nonepidermal gene expression programs. *Cbx4* ablation in mice results in a marked decrease of the epidermal thickness and keratinocyte (KC) proliferation associated with activation of numerous neuronal genes and genes encoding cyclin-dependent kinase inhibitors (p16/p19 and p57). Furthermore, the chromodomain- and SUMO E3 ligase–dependent Cbx4 activities differentially regulate proliferation, differentiation, and expression of nonepidermal genes in KCs. Finally, *Cbx4* expression in KCs is directly regulated by p63 transcription factor, whereas *Cbx4* overexpression is capable of partially rescuing the effects of p63 ablation on epidermal development. These data demonstrate that Cbx4 plays a crucial role in the p63-regulated program of epidermal differentiation, maintaining the epithelial identity and proliferative activity in KCs via repression of the selected nonepidermal lineage and cell cycle inhibitor genes.

Introduction

During development, tissue differentiation relies on the establishment of specific patterns of gene expression, which is achieved by lineage-specific gene activation and silencing in multipotent stem cells and their progenies (Slack, 2008; Blanpain and Fuchs, 2014). The program of epidermal differentiation in mice begins at about embryonic day 9.5 (E9.5) and results in the formation of an epidermal barrier by E18.5 (Koster and Roop, 2007; Blanpain and Fuchs, 2009). The process of terminal differentiation in epidermal cells is executed by sequential changes of gene expression in the keratin type I/II loci, followed by the onset of expression of the epidermal differentiation complex genes encoding the essential components of the epidermal barrier (Fuchs, 2007). This program is governed by the coordinated involvement of several transcription factors (p63, AP-1, Klf4, Arnt, etc.), signaling pathways (Wnt, Bmp, Hedgehog, EGF, Notch, FGF, etc.), and epigenetic regulators (DNA/histone-modifying enzymes, Polycomb genes, higher order and ATP-dependent chromatin remodelers, and noncoding and microRNAs) that control expression of lineage-specific genes (Khavari et al., 2010; Botchkarev et al., 2012; Frye and Benitah, 2012; Perdigoto et al., 2014).

Among these regulatory molecules, the p63 transcription factor serves as a master regulator of epidermal development and controls expression of a large number of distinct groups of genes (Viganò and Mantovani, 2007; Vanbokhoven et al., 2011; Botchkarev and Flores, 2014; Kouwenhoven et al., 2015). *p63* knockout (KO) mice fail to form stratified epithelium and express several epidermis-specific genes (Mills et al., 1999; Yang et al., 1999). In the epidermis, p63 regulates the expression of distinct chromatin-remodeling factors, such as Satb1 and Brg1, which, in turn, control the establishment of specific nuclear positioning and conformation of the epidermal differentiation complex locus required for full activation of keratinocyte (KC)-specific genes during terminal differentiation (Fessing et al., 2011; Mardaryev et al., 2014).

Epigenetic regulators exhibit both activating and repressive effects on chromatin in KCs: the histone demethylase Jmjd3, ATP-dependent chromatin remodeler Brg1, and genome

Correspondence to Vladimir A. Botchkarev: v.a.botchkarev@bradford.ac.uk or vladbotc@bu.edu

Abbreviations used in this paper: ANOVA, analysis of variance; ChIP, chromatin immunoprecipitation; ChIP-qPCR, ChIP–quantitative PCR; KC, keratinocyte; KO, knockout; LCM, laser capture microdissection; qRT-PCR, quantitative real time–PCR; WT, wild type.

Supplemental Material can be found at:
http://jcb.rupress.org/content/suppl/2015/12/23/jcb.201506065.DC1.html
http://jcb.rupress.org/content/suppl/2016/01/04/jcb.201506065.DC2.html

The Rockefeller University Press $30.00
J. Cell Biol. Vol. 212 No. 1 77–89
www.jcb.org/cgi/doi/10.1083/jcb.201506065

Published December 28, 2015

organizer Satb1 promote terminal KC differentiation, whereas the DNA methyltransferase DNMT1, histone deacetylases HDAC1/2, and Polycomb components Bmi1 and Ezh1/2 stimulate proliferation of the progenitor cells via repression of the genes encoding cell cycle inhibitors, as well as inhibiting premature activation of terminal differentiation–associated genes (Sen et al., 2008, 2010; Ezhkova et al., 2009; LeBoeuf et al., 2010; Fessing et al., 2011; Mardaryev et al., 2014).

Polycomb chromatin-remodeling proteins form two complexes (Polycomb repressive complex 1 and 2 or PRC1/2) that compact the chromatin and inhibit transcription by preventing binding of the transcription machinery to gene promoters (Simon and Kingston, 2013; Cheutin and Cavalli, 2014). Recent data reveal that binding of the noncanonical PRC1 complex containing histone demethylase KDM2B, PCGF1, and RING/YY1-binding protein (RYBP) promotes basal ubiquitylation of the H2A at lysine 119 (H2AK119) at unmethylated CpG-rich DNA regions, which is sufficient to recruit the PRC2 complex (Blackledge et al., 2014; Cooper et al., 2014; Kalb et al., 2014). The PRC2 component Ezh1/Ezh2 histone methyltransferase promotes trimethylation of H3K27, followed by targeting of the Cbx proteins as a part of the canonical PRC1 complex to H3K27me3, which result in further increase of the H2AK119 ubiquitylation catalyzed by the PRC1 component Ring1b (Simon and Kingston, 2013; Cheutin and Cavalli, 2014; Perdigoto et al., 2014; Schwartz and Pirrotta, 2014).

In the epidermis, the Polycomb components Bmi1, Ezh1/2, and Jarid2 stimulate proliferation of the progenitor cells via repression of the genes encoding cell cycle inhibitors, including the *INK4A–INK4B* locus, as well as inhibit premature activation of terminal differentiation–associated genes (Ezhkova et al., 2009; Mejetta et al., 2011). In addition, Ezh1/2 restricts differentiation of the epidermal progenitor cells by repressing the *Sox2* gene, which, in turn, promotes Merkel cell–specific differentiation (Bardot et al., 2013).

The *Cbx4* gene belongs to the PRC1 family and has a chromodomain interacting with the H3K27me3 histone mark and mediating transcriptional repression together with the PRC2 complex (Li et al., 2007; Luis et al., 2011). Cbx4 also possesses SUMO E3 ligase activity that promotes sumoylation of other proteins, including DNA methyltransferase Dnmt3a, thus providing a link between Polycomb-mediated gene silencing and DNA methylation (Li et al., 2007). In normal human skin, the Cbx4 protein protects epithelial stem cells from senescence through PRC-dependent repression of the *Ink4a* locus, as well as controls their differentiation through PRC-independent mechanisms (Luis et al., 2011). These data suggest Cbx4 as a critical determinant regulating the activity of stem cells and their progenies in the skin. However, its role in the control of epidermal development and in establishing tissue-specific gene expression patterns still remains unclear.

Here, we show that Cbx4 is a critical determinant regulating the establishment and maintenance of the epidermal differentiation program that represses nonepidermal lineage genes and controls cell proliferation/differentiation in the epidermis. We also show that Cbx4 serves as a direct p63 target and mediates its repressive effects on the expression of nonepidermal lineage genes and selected cell cycle inhibitor genes. These data illustrate how p63 transcription factor operates in concert with epigenetic regulator Cbx4 to establish and maintain the lineage-specific program in differentiating cells and in governing epithelial differentiation/function.

Results

Cbx4 expression is increased in the epidermal KCs during the stratification stage of epidermal development

To perform the genome-wide analysis of transcriptomes in epidermal progenitor cells during development, we used laser capture microdissection (LCM) and obtained RNA samples from the basal epidermal layer before and after the onset of epidermal stratification (E11.5 and E16.5, respectively), as well as postnatally at 1.5 d (P1.5) and 8 wk (P56, adult) as described previously (Sharov et al., 2006). Detailed analysis of the transcript levels of different Polycomb group genes revealed their dynamic expression during development of the mouse epidermis (Fig. S1 A and Table S1). Among the PRC1 genes, the *Cbx4* transcript and protein levels were strongly increased in the basal KCs during the transition from single-layered epithelium to stratified squamous epidermis (E11.5 vs. E16.5; Fig. 1, A and B; Fig. S1 A; and Table S1). Consistent with previous observations (Ezhkova et al., 2009), the onset of epidermal stratification (E11.5–E16.5) was also characterized by the highest levels of the PRC2 component *Ezh2* gene expressions in the basal KCs, followed by its decline at the later stages of epidermal differentiation (E16.5–P1.5; Fig. S1 A and Table S1).

Interestingly, Cbx4 protein expression was even higher in differentiating suprabasal KCs, whereas significantly lower expression levels were seen in the dermal compartment of the skin (Fig. 1, B and D). In contrast to *Cbx4*, other PRC1 genes showed a less pronounced increase, or even a decrease, in their expression levels at the early stages of epidermal development (Fig. S1 A). As the epidermis fully matured (P1.5), basal progenitor cells showed a decline in expression of most of the PRC1 genes except *Cbx7*, *Phc1*, and *Pcgf1* (Fig. S1 A and Table S1). Interestingly, Cbx4 expression levels also decreased in the basal KCs of adult skin compared with E16.5, but were still considerably higher than at E11.5 (Fig. 1 C, Fig. S1 A, and Table S1).

Cbx4 controls KC proliferation and terminal differentiation in the developing epidermis

To uncover the role of *Cbx4* in the epidermal progenitor cells during development, we used mice bearing an inactivation allele lacking the first two exons and a 0.9-kb upstream region of the *Cbx4* gene disrupting functional Cbx4 protein synthesis (Liu et al., 2013). The *Cbx4* homozygous KO mice were not viable and died within 1 h after birth because of some (not yet fully clear) developmental abnormalities, including thymic hypoplasia (Liu et al., 2013). Immunostaining analysis for Cbx4 confirmed the abolished protein expression in the skin of Cbx4KO compared with wild-type (WT) littermates (Fig. 1 B).

To explore the skin phenotype upon *Cbx4* ablation, we performed a histological assessment of the stratified skin epithelium at different developmental time points: E14.5, E16.5, and E18.5. At E14.5, *Cbx4*-null epidermis showed significantly reduced thickness correlated with a decreased number of stratified cellular layers and significant reduction in the number of proliferating $Ki67^+$ cells in the basal layer compared with WT controls (Fig. 1, E–H). Similar to E14.5, *Cbx4*-null epidermis remained significantly thinner and harbored fewer proliferating basal cells at E16.5, whereas such differences become insignificant at E18.5 (Fig. 1, E–H). At E16.5, the appearance of the senescence-associated marker γ-H2AX was seen in the epidermis of *Cbx4*KO mice,

Published December 28, 2015

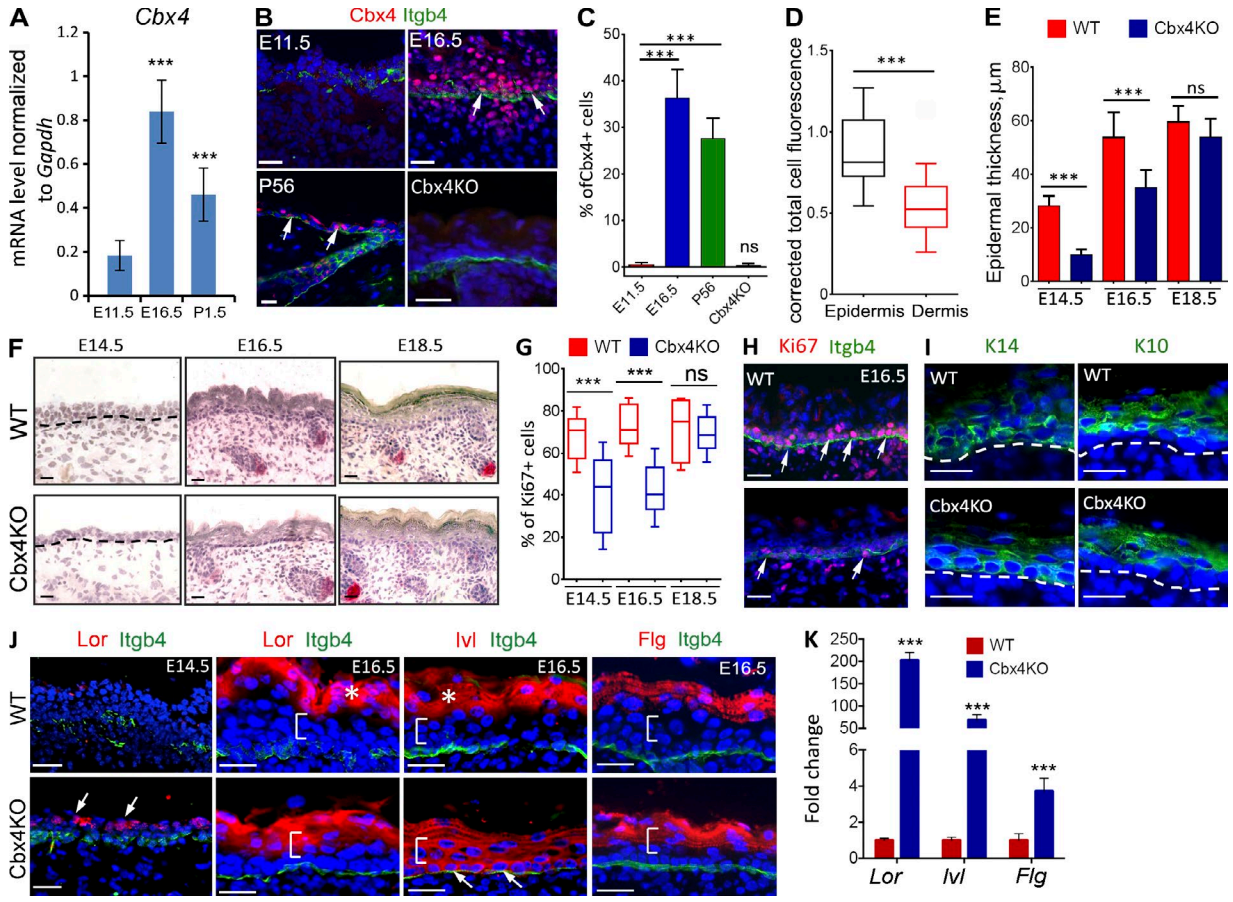

Figure 1. ***Cbx4*KO mice show a decrease of cell proliferation and premature terminal differentiation in the developing epidermis.** (A) *Cbx4* transcript expression in epidermal KCs at E11.5, E16.5, and P1.5 (qRT-PCR; mean ± SD; *n* = 3). (B) Cbx4 immunofluorescence is not detected in the E11.5 epidermis. In comparison to E11.5, Cbx4 levels are increased in basal and suprabasal KCs at E16.5, as well as in postnatal (P56) skin (arrows). Cbx4KO mice show a lack of Cbx4 expression in the epidermis. Integrin-β4 (Itgb4) expression outlines the basement membrane of the epidermis. DAPI counterstain (blue) shows the nuclei. (C) Quantification of Cbx4⁺ cells in the epidermis at different developmental stages in WT mice and in Cbx4KO skin (mean ± SD). *n* = 3. (D) Quantification of Cbx4 total cell fluorescence in both epidermal and dermal skin compartments of WT mice at E16.5 (box plot with 5–95% confidential intervals; the whiskers show minimum and maximum values). *n* = 3. (E and F) Histomorphological analyses of the alkaline phosphatase/hematoxylin-stained skin showed a reduced epidermal thickness in *Cbx4*KO mice compared with WT mice at E14.5 and E16.5 (mean ± SD). *n* = 3. Dashed lines separate epidermis and dermis. (G and H) Immunofluorescence detection (H) and quantification (G) of Ki67⁺ cells (H, arrows) showed reduced cell proliferation in the *Cbx4*KO epidermis versus WT counterpart at E14.5 and E16.5 (box plot with 5–95% confidential intervals). *n* = 4. Integrin-β4 expression outlines the basement membrane of the epidermis. (I and J) Immunofluorescence detection of K14 and K10 (I) and late (J) differentiation markers revealed premature onset of the terminal differentiation in the *Cbx4*KO epidermis (dashed lines indicate the epidermal/dermal border). In *Cbx4*KO mice, Loricrin protein was detected as early as E14.5, before onset of terminal differentiation in WT mice (J). At E16.5, Loricrin and Filaggrin were detected in early suprabasal cells, whereas Involucrin expression was up-regulated already in the basal progenitor cells (arrows). Brackets and asterisks depict the positions of the spinous and granular epidermal layers, respectively. (K) Increase of the *Lor*, *Ivl*, and *Flg* mRNA levels in the LCM-captured basal epidermal cells of E16.5 *Cbx4*KO mice versus WT controls (mean ± SD). *n* = 3. ***, P < 0.001. Bars, 25 µm. ns, not significant.

whereas immunostaining for active caspase 3 showed a lack of any changes in the KC apoptosis between WT and *Cbx4*KO mice (Fig. S3, E and F). The reduced proliferation of E16.5 basal epidermal KCs was associated with increased expression of the cell cycle inhibitor genes (senescence-linked *Ink4a* locus p16/p19 and *Cdkn1c*/p57 gene; Fig. S3, A and B), which are well-known targets of the Polycomb proteins in several tissues, including the skin (Ezhkova et al., 2009; Luis et al., 2011).

As CBX4 was previously shown to prevent terminal differentiation in human epidermal progenitor cells independently of its Polycomb-associated repressive function (Luis et al., 2011), we explored the effect of *Cbx4* ablation on the expression of early and late epidermal differentiation genes in the developing mouse epidermis. In the absence of *Cbx4*, cells of the embryonic ectoderm were able to acquire an epidermal fate and commence a differentiation program as indicated by positive K14 and K10 staining in the basal and suprabasal cells (Figs. 1 I and S4 A). However, Loricrin, a marker of terminally differentiating KCs, was prematurely expressed in the suprabasal cells located just above the basal cells in the Cbx4-deficient epidermis at E14.5, whereas its expression was not detectable in WT epidermis at this stage (Figs. 1 J and S4 A). In E16.5 WT embryos, the most superficial late suprabasal cells underwent terminal differentiation and expressed the key components of the cornified cell envelope such as Loricrin, Involucrin, and Filaggrin (Figs. 1 J and S4 A). In contrast to WT mice, the premature onsets of Loricrin, Involucrin, and Filaggrin expression were seen in the early suprabasal cells in E16.5 *Cbx4*KO mice (Figs. 1 J and S4 A). Immunofluorescence data on the expression of the markers of terminally differentiated KCs were in concordance with quantitative real time–PCR (qRT-PCR) data showing the markedly elevated levels of the *Lor*, *Inv*, and *Flg*

Published December 28, 2015

transcripts in the E16.5 epidermis of *Cbx4*KO mice versus WT controls (Fig. 1 K). Thus, Cbx4 suppresses the expression of terminal differentiation–associated genes in the basal progenitor cells during murine epidermal development.

Cbx4 represses nonepidermal lineage genes in KCs during epidermal development

Next, we analyzed the distribution of H2AK119Ub and H3K27me3, two key histone modifications associated with Polycomb-mediated gene repression, in the epidermis of *Cbx4*KO mice. According to the model of Polycomb-mediated gene silencing, a basal level of H2AK119 ubiquitylation at unmethylated CpG-rich DNA regions is maintained by noncanonical PRC1 complexes lacking the Cbx proteins, whereas one of the Cbx family members serving as a part of the canonical PRC1 complex is only involved in the subsequent step in the Polycomb-mediated gene silencing and is required for binding to H3K27me3, followed by the Ring1b-mediated further increase of the H2AK119 ubiquitylation over its basal level (Simon and Kingston, 2013; Cheutin and Cavalli, 2014; Perdigoto et al., 2014; Schwartz and Pirrotta, 2014).

In contrast to WT mice, epidermal cells in E14.5 and E16.5 *Cbx4*KO mice showed a significantly decreased level of H2AK119ub1 expression, which we considered as a basal level (Fig. 2, A and B). However, the expression levels of H3K27me3 were not changed in the epidermis of *Cbx4*KO mice compared with WT controls (Fig. 2, C and D). Also, expression of the histone methylase Kdm2b, a constituent of the noncanonical PRC1 complex (Schwartz and Pirrotta, 2014), was increased in the epidermis of *Cbx4*KO mice, whereas expression of Ring1b forming the canonical PRC1 complex together with Cbx4 and catalyzing the H2AK119 ubiquitylation was not changed (Fig. S2, A and B). Importantly, *Cbx4* ablation changed neither H2AK119ub1 nor H3K27me3 expression in the dermal cells (Fig. S2 C), thus suggesting epidermis-specific effects of Cbx4 on gene repression in the skin. These data were consistent with the data showing the significantly increased Cbx4 expression levels in the epidermis versus dermis in WT mice (Fig. 1 D) and suggested that, similar to other cell lineages, Cbx4 most likely mediates the recruitment of the canonical PRC1 complex to H3K27me3, followed by further ubiquitylation of H2AK119 over its basal levels mediated by PRC1 in epidermal cells.

Our data also demonstrate that the expression levels of H2AK119ub1 in the epidermis of E18.5 *Cbx4*KO and WT mice became quite similar (Fig. 2, A and B), which suggests that other Cbx proteins (Fig. S1 C) might substitute for Cbx4 in the canonical PRC1 complex in Cbx4KO mice. These data are also quite consistent with the data demonstrating that maximal differences in the epidermal thickness and proliferation between WT and *Cbx4*KO mice are seen at E16.5, whereas such differences become insignificant at E18.5 (Fig. 1, E–H).

To determine the molecular targets of Cbx4 in the epidermal KCs during development, we correlated a microarray transcript profiling from E16.5 LCM-captured *Cbx4*-deficient basal cells with Cbx4 chromatin immunoprecipitation (ChIP) sequencing (ChIP-seq) analyses performed on primary epidermal KCs isolated from E16.5 WT mice. About 13.8% of genes up-regulated in the basal epidermal cells from *Cbx4*KO mice showed Cbx4 ChIP-seq binding, thus likely representing direct Cbx4 targets in KCs (Fig. 2, E–G). Because the Cbx4 chromodomain binds to H3K27me3, which results in a further increase of the H2AK119 ubiquitylation over its basal levels catalyzed by the PRC1 component Ring1b (Li et al., 2007; Luis et al., 2011), we merged data for direct Cbx4 targets and ChIP-seq data for H3K27me3 and found that 60.9% of Cbx4 direct target genes in primary epidermal KCs show peaks for both Cbx4 and H3K27me3 within 100 kb of their transcription start sites (Fig. 2 E and Table S5). Furthermore, 12.1% of these genes showed the overlapping ChIP-seq peaks for Cbx4 and H3K27me3, thus pointing to these genes as direct targets for Cbx4-mediated repression (Table S5).

The DAVID bioinformatics tool for gene ontology functional annotation revealed an enrichment of the genes involved in the control of neuronal development among the Cbx4 targets (Fig. 2, F and G; and Table S5). In primary epidermal KCs, several neuronal and other lineage-specific genes (*Nefl*, *Neurog3*, *Mobp*, *En2*, and *Lhx4*) contained both Cbx4 and H3K27me3 ChIP-seq peaks in their regulatory regions (Fig. 2 H). Validation by qRT-PCR showed increased transcript levels of the selected Cbx4 target genes in the *Cbx4*-null epidermal cells (Fig. 2 I), including the *Nefl* and *Mobp* genes encoding a neurofilament light polypeptide and myelin-associated oligodendrocyte basic protein, structural components of the neurons, and Schwann cells, respectively (Montague et al., 1997; Jordanova et al., 2003). In addition, expression of the *Neurog3*, *Olig2*, *En2*, and *Lhx4* genes, encoding the corresponding transcription factors controlling the development of nervous system and some other non–KC cell lineages (Hobert and Westphal, 2000; Wallén and Perlmann, 2003; Pelling et al., 2011; Mitew et al., 2014), was markedly increased in the epidermis of *Cbx4*KO mice compared with WT controls (Fig. 2 I).

Interestingly, *Nefl* transcript levels showed an inverse correlation with *Cbx4* expression in the WT epidermis during E11.5–E16.5 (Figs. 1 A, 2 I, and S1 C). Further analysis revealed that, in addition to the dermal nerve fibers, an ectopic expression of the Nefl protein was seen in both basal and suprabasal epidermal layers of E16.5 *Cbx4*KO mice, whereas an exclusively neuronal Nefl expression was seen in WT mice (Fig. 2 J). Furthermore, ChIP–quantitative PCR (ChIP-qPCR) analyses showed enrichments for Cbx4, H2AK119ub1, and H3K27me3 at the regulatory region of the *Nefl* gene, whereas a lack of Cbx4 enrichment was seen at the regulatory region of the *Lor* gene that did not belong to the category of the Cbx4 direct targets and served as a control in this experiment (Fig. 2 K). In addition, shRNA-mediated Cbx4 gene silencing resulted in a significant decrease in the Cbx4 and H2AK119ub1 levels at the regulatory region of the *Nefl* gene in primary epidermal KCs, whereas the H3K27me3 levels were not changed (Figs. 2 L and S2 D). These data were consistent with the data demonstrating the decrease in the H2AK119ub1 levels in the epidermis of *Cbx4*KO versus WT mice (Fig. 2, A and B) and suggest that Cbx4 as a part of the canonical PRC1 complex facilitates repression of its target *Nefl* gene. However, *Cbx4* ablation did not affect Merkel cell numbers in the developing epidermis or expression of the transcription factors (Atoh1 and Sox2) involved in their differentiation (Fig. 4, B and C; and Table S5; Van Keymeulen et al., 2009; Bardot et al., 2013; unpublished data).

Chromodomain- and SUMO E3 ligase–dependent Cbx4 activities differentially regulate proliferation, differentiation, and expression of nonepidermal genes in KCs

As Cbx4 uniquely possesses, among PRC1-associated Cbx subunits, both Polycomb and non-Polycomb SUMO E3 ligase activities (Li et al., 2007; Luis et al., 2011), we next

Published December 28, 2015

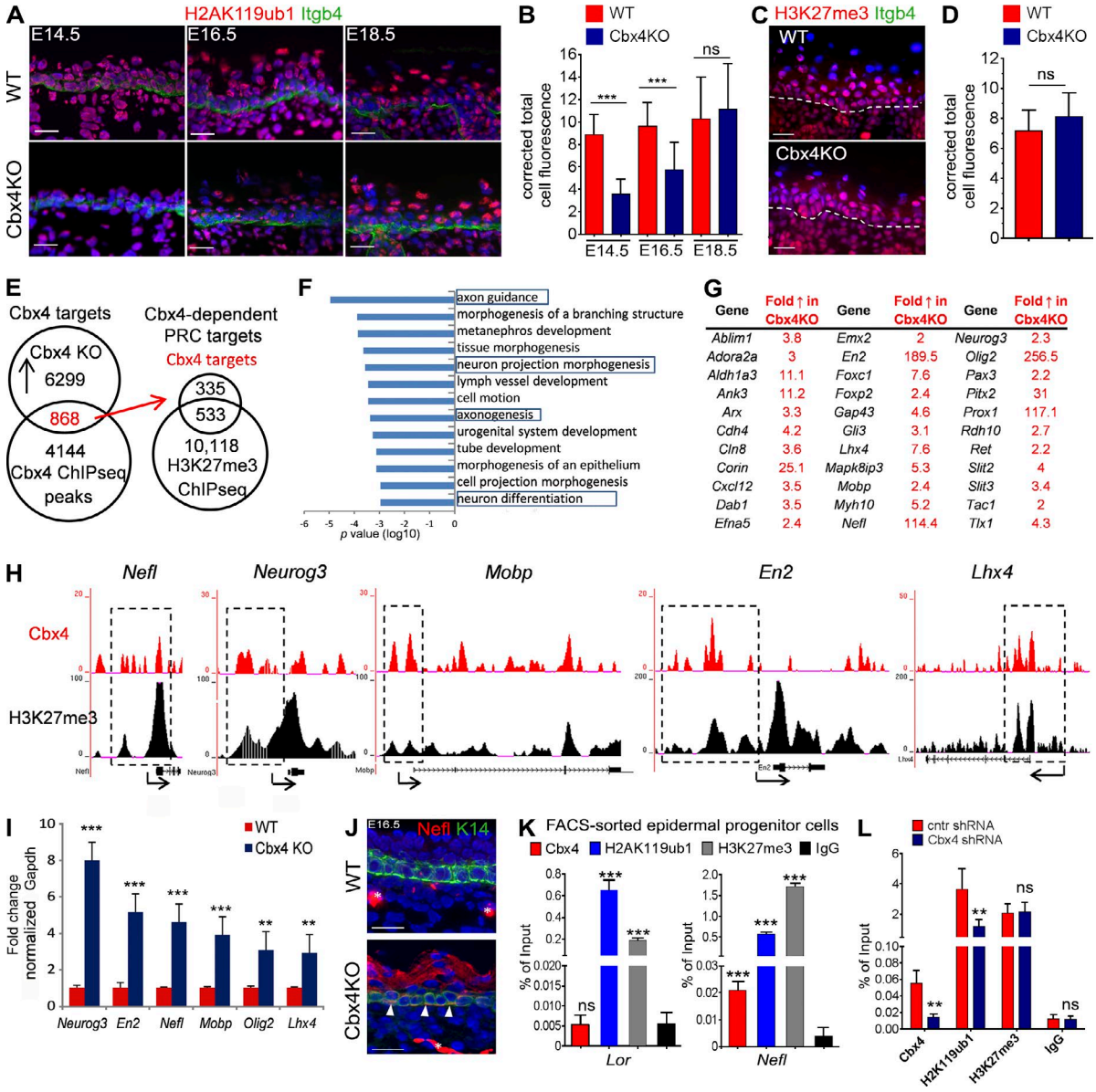

Figure 2. **Activation of nonepidermal lineage genes in Cbx4-deficient epidermis.** (A and B) Distribution and quantification of H2AK119ub1 immunofluorescence in WT and *Cbx4*KO skin. H2AK119ub1 is markedly reduced in the *Cbx4*KO epidermis at E14.5 and E16.5, whereas its expression is restored by E18.5. (C and D) Lack of changes in the cutaneous H3K27me3 expression between WT and *Cbx4*KO mice. Dashed lines separate epidermis and dermis. (E) Overlap of the Cbx4 and H3K27me3 ChIP-seq data with the expression arrays obtained from the epidermis of *Cbx4*KO versus WT mice depicts the direct Polycomb-dependent Cbx4 target genes in KCs that are up-regulated upon *Cbx4* ablation. (F) Ontology of the Cbx4 target genes using DAVID bioinformatic resources. The bars represent the log10 p-values of each category. (G) Selected Cbx4 target genes involved in neuronal development and/or functioning. (H) ChIP-seq tracks depicting Cbx4 and H3K27me3 binding to the selected target genes (a single representative experiment out of two repeats is shown). Dashed outlines depict the corresponding gene regulatory regions. (I) qRT-PCR validation of the selected *Cbx4* target genes up-regulated in the basal progenitor cells from *Cbx4*KO mice versus WT controls (mean ± SD). $n = 3$. (J) Ectopic Nefl protein expression in the *Cbx4*KO epidermis (arrowheads) compared with WT counterparts. Asterisks denote Nefl$^+$ dermal nerve fibers in the WT and *Cbx4*KO mice. (K) ChIP-qPCR shows Cbx4 binding to *Nefl* but not to *Lor* promoter regions. Both *Lor* and *Nefl* are enriched in H2AK119ub1 and H3K27me3 histone marks (mean ± SD). $n = 3$. (L) Cbx4 knockdown in primary mouse KCs with shRNA decreases Cbx4 binding and reduces the H2AK119ub1 enrichment on the *Nefl* promoter region (mean ± SD). $n = 3$. **, $P < 0.01$; ***, $P < 0.001$. Bars, 25 µm. ns, not significant.

questioned whether its effects on epidermal proliferation, differentiation, and repression of nonepidermal genes seen during murine skin development are associated with one of these Cbx4 activities. We infected primary epidermal KCs isolated from newborn WT mice with retroviral constructs expressing either WT *Cbx4* (*Cbx4*WT), chromodomain-mutated *Cbx4* (*Cbx4*CDM), or E3 ligase–deficient *Cbx4* (*Cbx4*ΔSIM; Luis et al., 2011).

Interestingly, transfection of cells with *Cbx4*WT or *Cbx4*CDM constructs did not show any effect on the number of proliferating Ki67$^+$ cells, whereas a prominent decrease in proliferation was seen in the cells expressing the E3 ligase–deficient *Cbx4*ΔSIM construct (Fig. 3, A and B). These data were consistent with the data showing the decrease of epidermal proliferation in *Cbx4*KO mice (Fig. 1, G and H) and suggest that the effects of Cbx4 on proliferation in cultured KCs are mediated predominantly by its E3 ligase domain.

Published December 28, 2015

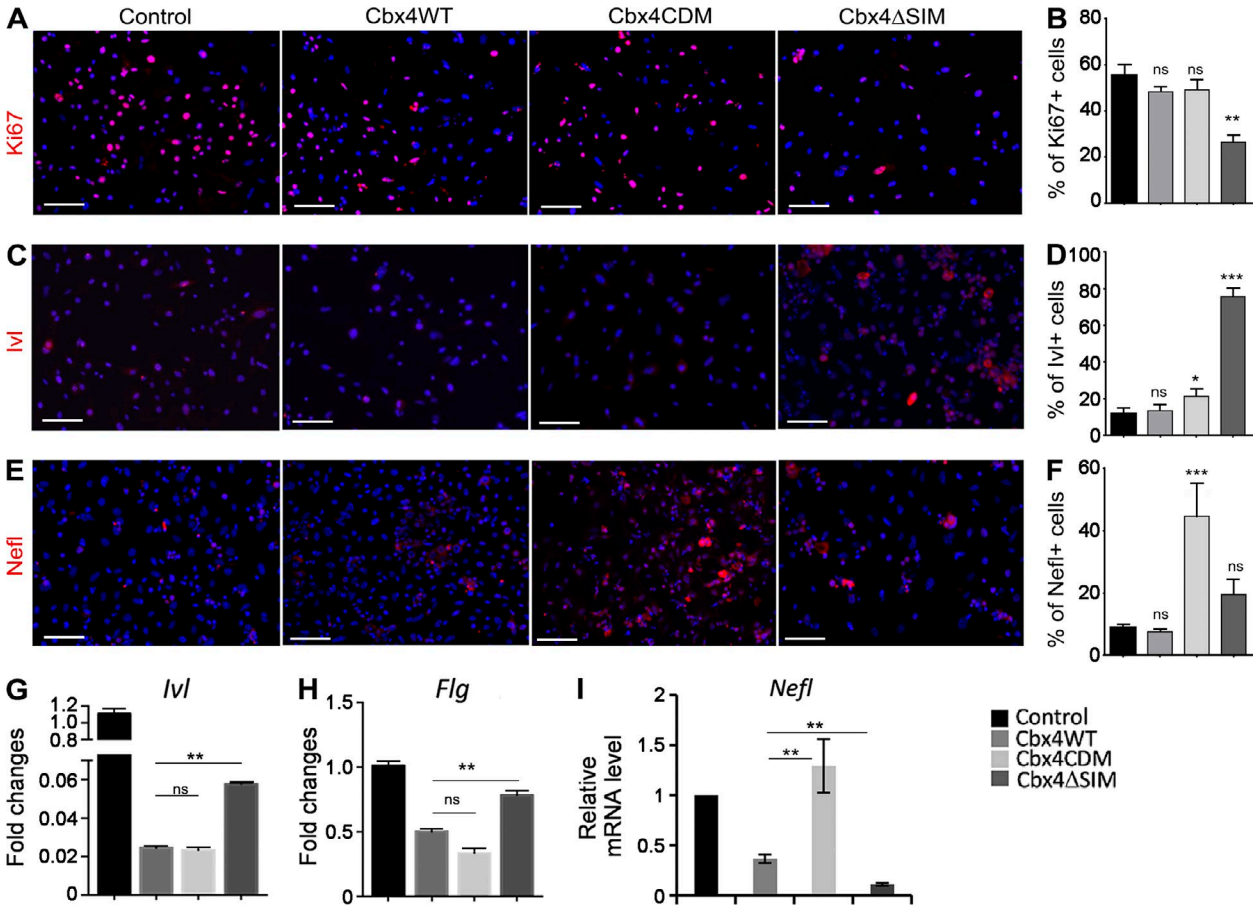

Figure 3. **SUMO E3 ligase– and chromodomain-dependent activities of Cbx4 in the epidermal progenitor cells.** (A–F) Immunofluorescent detection and quantification of Ki67 (A and B), Ivl (C and D), and Nefl (E and F) expression in the primary mouse KCs infected with *Cbx4*WT-, *Cbx4*CDM-, and *Cbx4*ΔSIM-expressing retroviruses. The number of Ki67$^+$-proliferating cells is significantly reduced, whereas Ivl expression is markedly increased in *Cbx4*ΔSIM-expressing KCs. In contrast, Nefl expression is up-regulated in *Cbx4*CDM-expressing cells (mean ± SD). $n = 3$. Bars, 50 µm. (G and H) qRT-PCR shows increased *Ivl* (G) and *Flg* (H) transcription in *Cbx4*ΔSIM-expressing cells (mean ± SEM). $n = 3$. (I) Increased levels of the *Nefl* transcripts in primary mouse KCs infected with *Cbx4*CDM-expressing retrovirus (mean ± SEM). $n = 3$. *, $P < 0.05$; **, $P < 0.01$; ***, $P < 0.001$. ns, not significant.

Given that Cbx4 suppresses senescence in human epidermal KCs (Luis et al., 2011), we examined the mechanisms underlying the Cbx4-dependent regulation of the senescence-linked cell cycle inhibitor genes and performed ChIP-qPCR analyses that revealed Cbx4 binding to the *Cdkn2a* (*p16/p19*) regulatory regions in primary epidermal KCs (Fig. S3 C). Transfection of primary epidermal KCs with *Cbx4*WT or *Cbx4*CDM constructs showed that the Cbx4 chromodomain is involved in regulating the expression of *Cdkn2a* and *Cdkn1c* (*p57*; Fig. S3 D). Together with our data demonstrating an increase in the expressions of p16/p19, p57, and the senescence marker γ-H2AX in the epidermis of *Cbx4*KO mice versus WT controls (Fig. S3, A, B, and E), these data demonstrated an involvement of the Cbx4 chromodomain in the control of expression of the senescence-associated *p16/p19* and *p57* genes. These data were in full concordance with the data of Luis et al. (2011) that show similar effects of the Cbx4 chromodomain on the expression of senescence-associated genes in human epidermal KCs.

To assess whether targeting of Cbx4 in the primary KCs affects cell differentiation, we analyzed the expression of two established terminal differentiation–associated markers (Involucrin and Filaggrin) after infection of cells with the WT or mutated *Cbx4*-expressing retroviruses. *Cbx4*WT-expressing cells showed a decrease in protein and gene expression of Involucrin in comparison with control cells (Fig. 3, C and D). However, *Cbx4*ΔSIM-treated KCs showed a prominent increase of Involucrin protein and gene expression compared with *Cbx*4WT- or *Cbx4*CDM-treated cells (Fig. 3, C, D, and G). Furthermore, transcripts of *Flg* were also increased upon *Cbx4*ΔSIM overexpression compared with the *Cbx4*WT and *Cbx4*CDM constructs (Fig. 3 H). Thus, similar to human epidermal progenitor cells (Luis et al., 2011), expression of terminal differentiation markers in mouse KCs occurs predominantly under the control of non-Polycomb SUMO E3 ligase activity of Cbx4.

To further elucidate which of the Cbx4 activities were likely responsible for repression of the nonepidermal lineage genes, we analyzed *Nefl* expression in the response to overexpression of the Cbx4 constructs harboring either chromodomain- or SUMO E3 ligase–mutated domains. A marked increase of both *Nefl* transcript and protein expression was detected in the *Cbx4*CDM-expressing cells compared with *Cbx*4WT and *Cbx4*ΔSIM (Fig. 3, E, F, and I). Thus, Cbx4 represses neuronal gene *Nefl* in epidermal KCs predominantly via the Polycomb-mediated inhibitory pathway.

Published December 28, 2015

Cbx4 is a direct p63 target mediating its inhibitory activity on nonepidermal genes in KCs

p63 is a major transcriptional regulator of epidermal development with multiple functions, including a direct positive transcriptional regulation of epidermal genes such as keratins and adhesion molecules (Koster and Roop, 2007; Vanbokhoven et al., 2011; Botchkarev and Flores, 2014; Kouwenhoven et al., 2015). A recent study has also highlighted an important role for p63 in suppression of nonepidermal lineage genes (De Rosa et al., 2009). To test whether p63-dependent suppression of the nonepidermal genes is mediated by Cbx4, we compared the transcriptomes of epidermal cells isolated by LCM from E18.5 *Cbx4*KO and *p63*KO embryos. A significant portion (34.7%) of the genes (716 out of 2,059) up-regulated in the p63-deficient KCs were also up-regulated in Cbx4KO basal epidermal cells, suggesting a functional link between p63 and Cbx4 (Fig. 4 A and Table S2). Furthermore, ChIP-seq analyses showed that 72 of these genes, including the *Nefl* gene, served as direct Cbx4 targets in KCs (Fig. 4 A and Table S2). The expression changes of the *Nefl* gene were further validated by qRT-PCR in *p63*-deficient KCs isolated from *p63*KO embryos and p63 siRNA–treated primary mouse KCs (Fig. 4, B and C). Similar to *Cbx4*KO epidermal cells, *p63*-deficient skin epithelial cells showed strongly up-regulated Nefl protein expression compared with WT cells (Fig. 4, D and E), further substantiating functional cooperation between p63 and Cbx4 in the repression of nonepidermal genes in the developing epidermal KCs.

To further investigate the relationships between p63 and Cbx4, we analyzed Cbx4 expression in *p63*KO embryonic skin. Both the Cbx4 transcript and protein levels were markedly reduced in the *p63*-deficient KCs (Fig. 4, F–H). Interestingly, in *p63*KO dermal cells, Cbx4 protein expression was detectable at similar levels to control mice (Fig. 4 G), suggesting a KC-specific *Cbx4* regulation by p63 transcription factor. By using a PatSearch tool (Grillo et al., 2003), we identified a highly conserved region ∼5.5 kb upstream of the *Cbx4* transcription start site containing several putative p63-binding sites (Fig. 4 I). Furthermore, ChIP revealed binding of the p63 transcription factor to the identified region in primary mouse KCs in vivo (Fig. 4 J). We cloned a 2.4-kb *Cbx4* 5′ UTR fragment, containing the putative p63-binding sites as an enhancer, into the pGl3 promoter plasmid (pGl3-*Cbx4*-luc) and coexpressed it with either ΔN*p63*-expressing or empty vector in the immortal KC HaCaT cell line. A marked increase in luciferase activity was seen in cells coexpressing pGl3-*Cbx4*-luc with pΔN*p63* vectors compared with a control plasmid (pFLAG-CMV2; Fig. 4 K), thus showing a direct transcriptional regulation of *Cbx4* by p63 in KCs.

Ectopic Cbx4 expression partially rescues the epidermal phenotype in embryonic skin explants of p63-deficient mice

To assess whether the restoration of Cbx4 expression is capable of partially rescuing the skin phenotype of *p63*KO mice, E13.5 skin explants isolated from *p63* heterozygous ($p63^{+/-}$) mice were cultured ex vivo and infected with *p63* shRNA–expressing lentiviruses in combination with either *Cbx4*-expressing or control lentiviruses (Fig. 5, A–E). Compared with the $p63^{+/-}$ skin explants treated with control viruses, treatment with *p63* shRNA in combination with control lentiviruses resulted in a marked decrease of the epidermal thickness, cell proliferation, and expressions of epidermal keratins K14 and K10, thus reproducing in part the skin phenotype of *p63*KO mice (Fig. 5, A–E). However, cotreatment of $p63^{+/-}$ skin samples with *p63* shRNA– and *Cbx4*-expressing lentiviruses resulted in a significant increase of epidermal thickness, cell proliferation, and K14/K10 expression compared with the samples treated with *p63* shRNA and control lentiviruses (Fig. 5, A–E). The restoration of epidermal proliferation after ectopic Cbx4 expression was consistent with data showing reduced cell proliferation in the epidermis of *Cbx4*KO mice compared with WT controls (Fig. 1, G and H). Furthermore, the Nefl protein was strongly decreased in the epithelium of p63-deficient embryonic skin explants transduced with Cbx4 (Fig. 5, D and E), suggesting that Cbx4 is indeed capable of inhibiting its expression in epidermal KCs ex vivo. Therefore, Cbx4 plays a role in mediating the p63-dependent program of gene repression during epidermal development and is capable of partially restoring the epidermal phenotype of p63-deficient mice.

Discussion

Polycomb-dependent transcriptional repression is a powerful mechanism that shapes gene expression programmers in essentially all cell types of living organisms during development and postnatal homeostasis, whereas alterations in the patterns of Polycomb-dependent gene repression contribute to many pathological conditions including carcinogenesis (Simon and Kingston, 2013). Polycomb PRC1 and PRC2 are multiprotein complexes, and despite the fact that the role of some Polycomb genes, such as Ezh1/2, in execution of terminal differentiation programmers in the epidermis and hair follicles was shown previously (Ezhkova et al., 2009, 2011), the effects of the other PRC1/2 components on the establishment of lineage-specific patterns of gene repression during skin development and epidermal differentiation remain unclear. Here, we show that PRC1 component Cbx4 plays a unique role in the establishment and maintenance of the KC lineage identity and represses nonepidermal lineage (neuronal) genes in the epidermal progenitor cells, as well as controls proliferation and inhibits premature differentiation in basal epidermal KCs.

We demonstrate that among different PRC1 genes, *Cbx4* shows the most prominent changes in its expression in the embryonic epidermis during its stratification, where Cbx4 is seen in basal and suprabasal KCs. Genetic *Cbx4* ablation results in a marked decrease of epidermal thickness and proliferation, as well as in the premature appearance of the terminal differentiation markers in the immediate suprabasal epidermal cells. Interestingly, *Ezh2*KO mice also show a decrease of epidermal proliferation and premature terminal differentiation (Ezhkova et al., 2009). Similar to *Ezh2*KO mice (Ezhkova et al., 2009), *Cbx4*-null mice show an increase of the *p16*/*p19* and *p57* cell cycle inhibitor genes in the epidermis, which, at least in part, explains the stimulatory effects of Cbx4 on epidermal proliferation. However, in contrast to *Ezh2*KO mice, *Cbx4* genetic ablation results in a marked decrease of the epidermal thickness, suggesting that Cbx4 plays a unique yet partially overlapping role with Ezh2 in the control of epidermal development.

The decreased cell proliferation observed in the epidermis upon *Cbx4* ablation is consistent with our previous results that show reduced cell proliferation and thymus hypoplasia in *Cbx4*KO mice (Liu et al., 2013). In contrast to other Cbx proteins, Cbx4 uniquely possesses both Polycomb and non-Polycomb

Published December 28, 2015

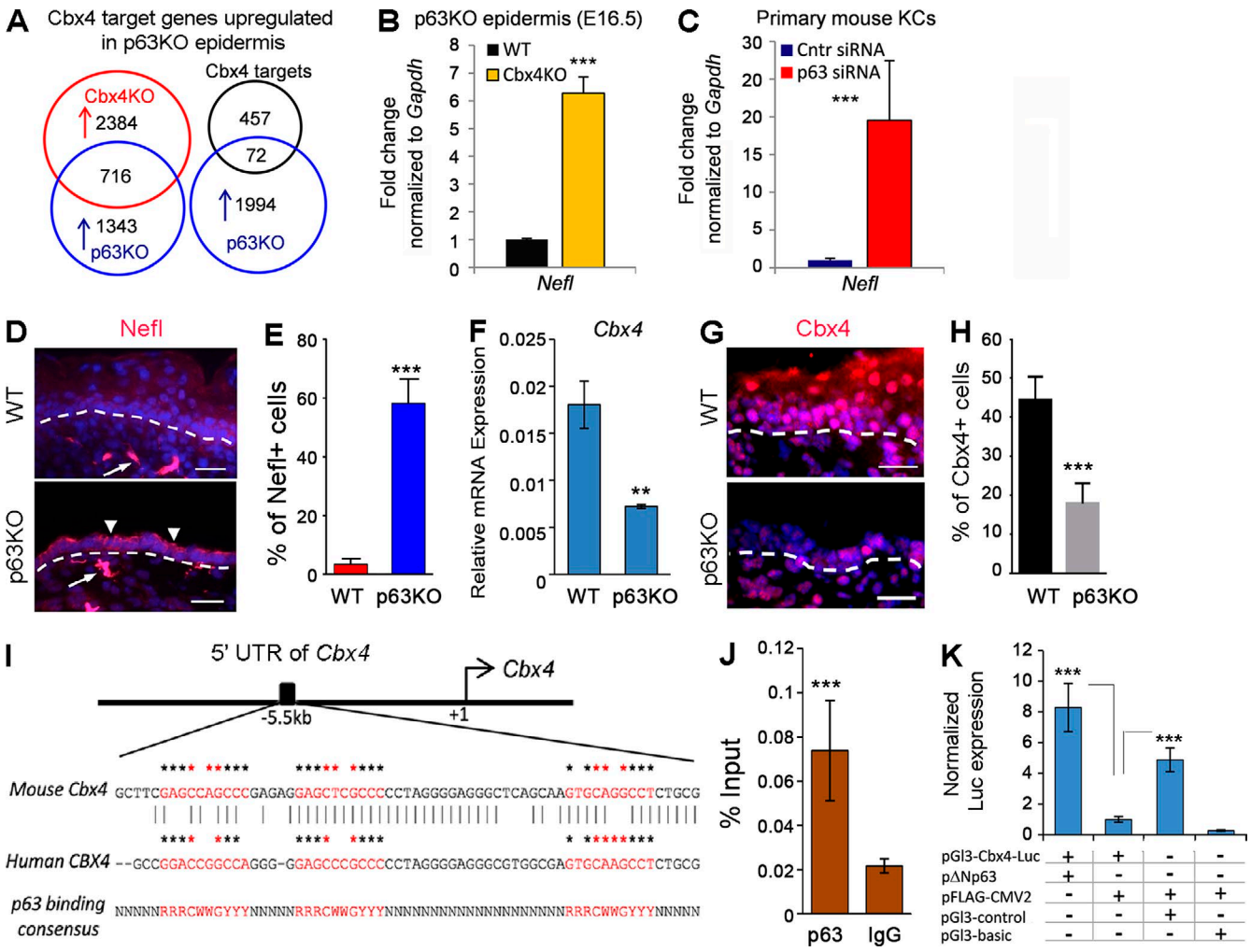

Figure 4. ***Cbx4* serves as a direct p63 target in epidermal KCs.** (A) Overlap of the Cbx4 target genes commonly up-regulated in laser-captured epidermis of E16.5 *Cbx4*KO and *p63*KO mice. (B and C) qRT-PCR validation of *Nefl* gene up-regulation in the epidermal progenitor cells *in p63*KO mice (B) and primary epidermal KCs expressing p63 shRNA (C; mean ± SD). *n* = 3. (D) Increased Nefl protein expression in the epidermis of *p63* mutant mice (arrowheads). Nefl-expressing dermal nerve fibers are shown by arrows. Dashed lines separate epidermis and dermis. (E) The number of Nefl+ epidermal cells is significantly increased in *p63*KO mice (mean ± SD). *n* = 3. (F and G) Cbx4 transcript (F) and protein (G) are markedly down-regulated in the epidermis of *p63*KO mice (mean ± SD). *n* = 3. Dashed lines separate epidermis and dermis. (H) A significant reduction in the number of Cbx4+ cells in *p63*KO skin compared with WT skin (mean ± SD). *n* = 3. (I) Conserved putative p63-binding sites are identified by the PatSearch tool in the mouse and human *Cbx4* 5′ UTR. Asterisks indicate consensus sequences for p63-binding sites, and core sequence elements are indicated by red asterisks. (J) ChIP-qPCR showing p63 binding to the identified region in the mouse *Cbx4* 5′ UTR. (K) A 2.4-kb region in the *Cbx4* 5′ UTR increases minimal SV40-promoter activity (pGl3-*Cbx4*-luc) upon coexpression with a ΔN*p63*-expressing construct compared with an empty plasmid (pFLAG-CMV2). Bars, 25 µm. **, P < 0.01; ***, P < 0.001.

SUMO E3 ligase activities (Li et al., 2007; Luis et al., 2011). We show here that in cultured primary epidermal KCs, only the non-Polycomb E3 ligase–deficient *Cbx4* (*Cbx4*ΔSIM) is capable of inhibiting proliferation, suggesting that the SUMO E3 ligase activity of Cbx4 contributes to the alterations of epidermal proliferation in *Cbx4*KO mice.

Interestingly, KCs treated with *Cbx4*ΔSIM also show a marked increase in the expression of terminal differentiation–associated markers, such as Involucrin or Filaggrin, thus suggesting that non-Polycomb SUMO E3 ligase Cbx4 activity might also inhibit the premature activation of terminal differentiation genes in the epidermis. These data are consistent with data demonstrating an involvement of SUMO E3 ligase Cbx4 activity in inhibiting differentiation in human epidermal progenitor cells (Luis et al., 2011). However, additional analyses are required to fully understand the mechanisms underlying the effects of the SUMO E3 ligase domain of Cbx4 in regulating gene expression in KCs.

Our data also reveal that the Cbx4 chromodomain is involved in the repression of the senescence-associated *Cdkn2a* gene, whereas *Cbx4* ablation results in the accumulation of H2AX as one of the senescence markers (Turinetto and Giachino, 2015) in epidermal KCs. These data are in full concordance with the data of Luis et al. (2011) that show similar effects of the Cbx4 chromodomain on the expression of senescence-associated genes in human epidermal KCs.

Histone methyltransferase Ezh2 catalyzing H3K27 trimethylation plays an important role in the prevention of premature activation of terminal differentiation genes in basal epidermal KCs (Ezhkova et al., 2009). The Cbx4 chromodomain mediates the targeting of the canonical PRC1 complex to H3K27me3, leading to the increase of H2AK119 ubiquitylation over its basal levels catalyzed by the PRC1 component Ring1b (Simon and Kingston, 2013; Cheutin and Cavalli, 2014; Perdigoto et al., 2014; Schwartz and Pirrotta, 2014). Although

Published December 28, 2015

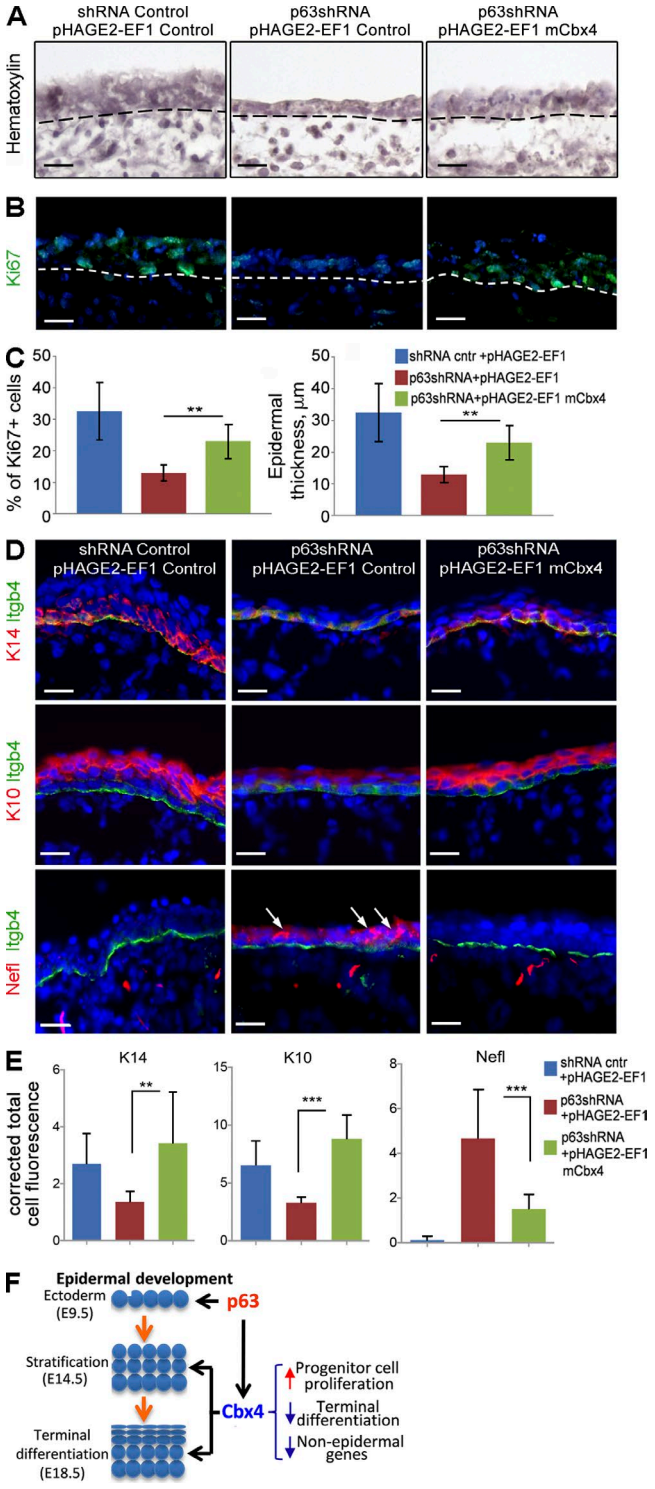

Figure 5. **Cbx4 partially rescues an epidermal phenotype in p63KO mice.** (A and B) Hematoxylin/AP staining (A) and immunodetection of Ki67$^+$-proliferating cells (B) in E13.5 ex vivo embryonic skin explants of heterozygous *p63*$^{+/-}$KO mice treated with p63 shRNA– and Cbx4-expressing lentiviruses. Dashed lines separate epidermis and dermis. (C) Cbx4 overexpression in *p63*-deficient epidermal cells significantly increases epidermal thickness and cell proliferation (mean ± SD). $n = 3$. (D and E) Quantitative immunofluorescence stainings with anti-K14, anti-K10, and anti-Nefl antibodies show down-regulation of K14/K10 and up-regulation of Nefl (arrows) in the epithelium of p63-deficient skin explants. Cotreatment of the explants with p63 shRNA– and Cbx4-expressing lentiviruses results in up-regulation of K14/K10 expression and down-regulation of Nefl expression in p63-deficient epidermis. Integrin-β4 (Itgb4) expression outlines the basement membrane of the epidermis. DAPI counterstain (blue) shows the nuclei (mean ± SD). $n = 3$. **, $P < 0.01$; ***, $P < 0.001$. (F) Scheme summarizing the p63-/Cbx4-mediated effects on gene repression in the developing epidermis. Bars, 25 µm.

the levels of H3K27me3 were not altered in the epidermis of *Cbx4*KO mice, *Cbx4* ablation resulted in a marked decrease in H2AK119Ub in the epidermis (presumably to its basal levels) compared with WT controls. The fact that *Cbx4*-null mice showed reduced levels of H2AK119Ub only in the epidermis, whereas H2AK119Ub levels in the dermal cell were not altered upon *Cbx4* ablation compared with WT controls, points to the specificity of this interaction.

Interestingly, *Cbx4* ablation is also accompanied by an increase of epidermal expression of Kdm2b histone demethylase that forms a noncanonical PRC1 complex together with PCGF1 and RYBP and promotes basal ubiquitylation of H2AK119 at unmethylated CpG-rich DNA regions (Blackledge et al., 2014; Cooper et al., 2014; Kalb et al., 2014). These data suggest that interaction of the noncanonical PRC1 complex with gene targets is likely not altered in the epidermis of *Cbx4*KO mice and that the Cbx4 chromodomain is specifically involved in the execution of the canonical PRC1-mediated gene repression in the epidermis via interaction with H3K27me3 followed by H2AK119 ubiquitylation.

However, a correlation between the Cbx4 and Ezh1/2 ChIP-seq targets in epidermal KCs might help in addressing the roles for PRC1 and PRC2 complexes in repressing the activities of the distinct gene groups in KCs. Our data reveal a contribution of the Cbx4 chromodomain to the repression of non-KC lineage (neuronal) genes in the epidermis, which is quite consistent with the data obtained from the *Ezh2*KO mice (Ezhkova et al., 2009). By merging the microarray data obtained from the epidermis of *Cbx4*KO mice with Cbx4 ChIP-seq and H3K27me3 ChIP-seq data, we demonstrate an enrichment of the genes associated with nervous system development among the direct Cbx4 targets in KCs. We show that several key genes encoding structural components of the neurons and Schwann cells (*Nefl* and *Mobp*) and transcription factors involved in the control of nervous system development (*Neurog3*, *Olig2*, *En2*, and *Lhx4*) are up-regulated in the epidermis of *Cbx4*KO mice compared with WT controls.

Epidermal and neuronal lineages share the common ectodermal origin (Patthey and Gunhaga, 2011; Benitah and Frye, 2012), and mechanisms that control gene repression during specification of these two lineages in the embryo are unclear. Ezh2 is strongly expressed in neural stem cells and is down-regulated during their differentiation into neurons and astrocytes, whereas its expression is increased during neural stem cell differentiation into the oligodendrocyte lineage (Sher et al., 2008). Analyses of the Ezh2 targets in neural stem cells (Sher et al., 2012) reveal that several genes encoding transcription factors involved in the control of nervous system development (*En2*, *Lhx4*, *Olig2*, *Pax3*, and *Pitx2*) also represent the direct Cbx4 targets in epidermal KCs. These data support an idea that Cbx4, through its chromodomain, and Ezh2 operate in concert to repress neuronal genes and maintain the epithelial fate in the epidermal progenitor cells, whereas Ezh2 also represses their differentiation into the Merkel cell lineage independently of Cbx4 (Bardot et al., 2013).

Specification and differentiation of the epidermal progenitor cells during development is supported by the p63 transcription

Published December 28, 2015

factor that serves as a master regulator of epidermal development (Koster and Roop, 2007; Vanbokhoven et al., 2011; Botchkarev and Flores, 2014; Kouwenhoven et al., 2015). Increased evidence demonstrates that p63 regulates several components of the epigenetic machinery (Brg1, Lsh, and Satb1) to regulate chromatin remodeling and establish the epidermal differentiation program (Fessing et al., 2011; Keyes et al., 2011; Mardaryev et al., 2014).

We show here that p63 also operates as a direct upstream regulator of *Cbx4*, which mediates its effects on cell proliferation and is involved in the repression of non-KC lineage genes. We showed previously that p63 directly interacts with Cbx4 in thymocytes, suggesting a possibility for both proteins to form a transcription complex to regulate expression of target genes (Liu et al., 2013). Consistently, comparison of the microarray data from the skin epithelium of *p63*KO mice and epidermis of *Cbx4*KO mice reveals that ∼35% of the genes up-regulated in the skin epithelium of *p63*KO mice are also up-regulated in the epidermis of *Cbx4* mutants, whereas ∼10% of these genes represent direct Cbx4 targets in KCs. Furthermore, we show that Cbx4 expression is markedly decreased in the skin epithelium of *p63*KO mice, p63 shows binding to the *Cbx4* regulatory region and stimulates *Cbx4* promoter activity, and Cbx4 is capable of partially rescuing alterations of KC proliferation upon p63 ablation in skin organ cultures.

Collectively, these data provide compelling evidence that Cbx4 operates as an important part of the p63-regulated program of establishing and maintaining epithelial cell fate in epidermal progenitors and that Cbx4-mediated repression of non-KC lineage genes serves as a crucial component of this program (Fig. 5 F). However, additional analyses are required to fully understand the complexity of Cbx4-dependent gene repression in epidermal KCs. In particular, the role of Cbx4 in the repression of other lineage-specific genes, including mesodermal genes in KCs, and the potential contribution of these genes in the control of epithelial–mesenchymal transition need to be carefully explored. Also, the roles of other members of the Cbx family, including Cbx6 and Cbx7, which might substitute for Cbx4 in the canonical PRC1 complex and partially compensate for the effects of Cbx4 ablation in epidermal KCs, need to be clarified.

Because skin contains a large variety of the progenitor cells for distinct cell lineages (epithelial, neuronal, and mesenchymal; Hunt et al., 2009), future research in this direction will shed light on the role of distinct Cbx family members in the control of progenitor cell differentiation and/or reprogramming isolated from the skin. This will also help to design novel approaches for modulating gene expression programmers in healthy and diseased skin via targeting the activity of Cbx genes.

Materials and methods

Animals and tissue collection

All animal studies were performed under protocols approved by a Home Office Project License. C57BL/6 mice were purchased from Charles River. Skin samples were collected from mice at distinct days of embryonic and postnatal development (E11.5, E14.5, E16.5, E18.5, P1.5, and P56). p63KO embryos were obtained by breeding $p63^{+/-}$ animals purchased from The Jackson Laboratory. Generation of Cbx4KO mice was described previously (Liu et al., 2013). In brief, the N-terminal region of the *Cbx4* gene including the first two exons and a 0.9-kb upstream region was targeted for *Cbx4* gene disruption. The null allele was gained upon Cre-loxP excision by crossing mice carrying the floxed allele with EIIa-Cre transgenic mice to achieve global gene KO, and the mice were bred on the C57BL/6J-129Sv genetic background. Genotyping of mice was performed using PCR, as described previously (Liu et al., 2013). For each developmental stage, six to seven samples were collected. Tissue samples were snap frozen in liquid nitrogen, embedded into optimal cutting temperature medium (VWR), and processed for immunofluorescent or LCM and microarray analyses as described in the following paragraph.

LCM, microarray, and qRT-PCR analysis

LCM of mouse basal KCs at selected stages of development was performed followed by RNA isolation, amplification, and microarray analysis as previously described (Sharov et al., 2006, 2009). In brief, 8-µm-thick frozen skin cryosections were dehydrated to preserve RNA integrity, and LCM was performed from the epidermis of WT, Cbx4KO, and p63KO mice at E11.5, E16.5, P0.5, and P56 using an LCM system (Arcturus; Life Technologies). Total RNAs were isolated using an RNA isolation kit (PicoPure; Life Technologies) followed by two rounds of linear RNA amplification using an RNA amplification kit (RiboAmp; Life Technologies). Equal amounts of RNA from each sample were labeled by Cy3 using a fluorescent labeling kit (Agilent Technologies). Quality and size distribution of the targets was determined by an RNA 6000 Nano Lab-on-a-chip assay (Agilent Technologies), and quantification was determined using a microscale spectrophotometer (NanoDrop). After one round of linear amplification in all analyses, Universal Mouse Reference RNA (Agilent Technologies) was used as a control. All microarray analyses were performed by MOgene, LC, using the 41K Whole Mouse Genome 60-mer Oligo Microarray kit (Agilent Technologies). All microarray data were normalized to the corresponding data obtained from the reference RNA. Two independent datasets were obtained from WT and transgenic mice, and p-values were calculated by Feature Extraction software (version 7.5; Agilent Technologies) using distribution of the background intensity values to signal intensity and using a Student's *t* test.

For qRT-PCR analysis of RNA isolated and amplified after LCM, PCR primers were designed on Beacon Designer software (PREMIER Biosoft International; Table S3). RT-PCR was performed using iQ SYBR green Supermix and the MyiQ Single-Color Real-Time PCR Detection System (Bio-Rad Laboratories). Differences between samples and controls were calculated using the Gene Expression Macro program (Bio-Rad Laboratories) based on the ΔΔCt equitation method with glyceraldehyde 3-phosphate dehydrogenase and peptidylprolyl isomerase A genes as internal housekeeping controls.

Plasmids

Cbx4WT and Cbx4-mutated retroviral plasmids (Cbx4CDM and Cbx4ΔSIM) were previously validated (Luis et al., 2011). In brief, Cbx4 cDNA was cloned into pMSCV and pMSCV-Puro-IRES-GFP. The chromodomain was mutated using the QuikChange II XL Site-Directed Mutagenesis kit (Agilent Technologies) to create the F11A and W35L double mutants. In Cbx4ΔSIM plasmid (a gift from D. Wotton, University of Virginia, Charlottesville, VA), Cbx4 cDNA was mutated to harbor internal deletion of nucleotides at the 784–795 and 1,381–1,404 positions, corresponding to both SIM1 (IVIV) and SIM2 (EVILLDSD) amino acid sequences, respectively (Merrill et al., 2010). Cbx4 knockdown was done using a validated shRNA construct (5′-CCGGCGACACCAGTAACCTTGGTATCTCGAGATACCAAGGTTACTGGTGTCGTTTTTG-3′) cloned into pLKO.1-GFP lentiviral plasmid (Morey et al., 2012). pGIPZ–p63 shRNA lentiviral plasmid (V3LMM_508694; GE Healthcare) contains a 5′-TGATCTTCAGCAACATCTC-3′ sequence and was used to target p63. pHAGE2-EF1-mCbx4 lentiviral plasmid was produced by cloning PCR-amplified mouse Cbx4 cDNA into pHAGE2-EF1 vector (a gift from G. Mostoslavsky, Boston University, Boston, MA).

Published December 28, 2015

Production of the Cbx4 and p63 expression and knockdown viruses

Cbx4WT-, Cbx4CDM-, and Cbx4ΔSIM-expressing retroviruses were produced by transfection of Phoenix-E/HEK293T packaging cells. Cbx4 shRNA– and p63 shRNA–expressing lentiviruses were produced by cotransfection of HEK293T cells with pLKO.1-EGFP-Cbx4 shRNA or pGIPZ–p63 shRNA and packaging (psPAX2) and envelope (pMD2.G) plasmids. For Cbx4-expressing lentiviruses, HEK293T cells were cotransfected with pHAGE2-EF1-mCbx4 and helper plasmids (pTAT, pREV, pHagp2(GAG/Pol), and pVSV-G) as published elsewhere (Mostoslavsky et al., 2005). For Cbx4-mutated retroviruses, Phoenix-E cells were transfected with pMSCV-PIG-CBX4-WT, pMSCV-PIG-CBX4-CDM, and pMSCV-PIG-CBX4-ΔSIM plasmids as published previously (Luis et al., 2011). Cell culture medium containing viruses was collected 24 h, 48 h, and 78 h after transfection, followed by precipitation of the viral particles using PEG-it solution (System Biosciences) as per the manufacturer's protocol.

Primary mouse KC culture

Epidermis from newborn C57BL/6 was separated from dermis by overnight digestion with 0.25% trypsin at 4°C. Epidermal sheath was added to prechilled, supplemented, low-calcium KC culture medium (MEM, 4% FBS, 0.05-mM $CaCl_2$, 0.4 µg/ml hydrocortisone, 5 µg/ml insulin, 10 mg/ml EGF, 10^{-10}-M cholera toxin, 2×10^{-9} T3, 2-mM L-glutamine, 100 U/ml penicillin, and 100 µg/ml streptomycin). To make a single-cell suspension, the epidermal tissue was chopped with scissors and triturated, followed by filtering through a 70-µM silicon strainer and plating onto collagen-coated plates and coverslips. Primary cells were grown in the KC culture medium at 33°C and 5% CO_2 until 60–70% confluent and infected with the retroviral/lentiviral particles. Cells were collected for subsequent qRT-PCR or immunofluorescent analyses 48 h after infection.

FACS

A single-cell suspension of newborn epidermal KCs was prepared as described in the previous paragraph. To ensure analysis and sorting of viable cells with intact chromatin, KCs were stained with UV Live/Dead Fixable Dye (Life Technologies) for 30 min on ice before fixation with 1% PFA for 10 min at RT. Fixed cells were labeled with CD49f-phycoerythrin and Sca-1–FITC antibodies (Table S4) for 1 h on ice. $CD49f^+/Sca\text{-}1^+$ basal KCs were gated after exclusion of dead cells and sorted on a cell sorter (MoFlo XDP; Beckman Coulter) as described elsewhere (Jensen et al., 2010). Sorted cells were pelleted at 2,000 *g* and stored at −80°C.

Luciferase reporter assay

To make the pGl3-Cbx4-luc plasmid, a 2.4-kb Cbx4 enhancer region (−5,954/−3,523 bp upstream of the Cbx4 transcription start site) was PCR amplified from genomic DNA and cloned into the Luciferase reporter plasmid pGl3 promoter (Promega) at BamHI–SalI sites using the In-Fusion HD Cloning System (Takara Bio Inc.). For the reporter assay, HaCaT cells were seeded into white-bottomed/white-walled 96-well plates at 10,000 cells/well, and transfections were performed after overnight incubation at 37°C. Cells were transfected with 200 ng DNA total plus 10 ng pRLTK Renilla Control vector (Promega): 100 ng pGl3-Cbx4-luc and 100 ng pΔNp63 or empty pFLAG-CMV2 vectors. After 48 h of incubation at 37°C, cells were washed with PBS, and the assay was performed using the Dual-Glo Luciferase Assay System (Promega) according to the manufacturer's protocol. Firefly luciferase activity was normalized against the Renilla luciferase activity, and the data represent three independent triplicates.

Histology and immunohistochemistry

For histology and histomorphometry, 8-µm cryosections were fixed in 4% PFA for 10 min at RT followed by hematoxylin staining and AP activity visualization using histoenzymatic reaction (Botchkareva et al., 1999, 2000; Ahmed et al., 2011, 2014). Epidermal thickness was measured in 10 microscopic fields using ImageJ software (National Institutes of Health). For immunohistochemistry, 8-µm cryosections were fixed in 4% PFA for 10 min at RT and incubated with primary antibodies (Table S4) overnight at 4°C, followed by application of corresponding Alexa Fluor 488 and Cy-555–coupled secondary antibodies (1:200; Life Technologies) for 60 min at 37°C. Cell nuclei were visualized with 4′6′-diamidino-2-phenylindol. Images were acquired on a microscope (Eclipse 50i; Nikon) with 20×/0.50 NA and 40×/0.75 NA Plan Fluor objectives (Nikon) using a digital camera (ExiAqua; QImaging) and Image-Pro Express 6.3 image analysis software (QImaging).

Comparative analysis of $Ki67^+$, Ivl^+, $Nefl^+$, and $Cbx4^+$ cells was done by evaluating the ratio of the number of positive cells to $DAPI^+$ cells, as descried previously (Sharov et al., 2003, 2005; Mardaryev et al., 2011). For quantification of $Ki67^+$ and $Cbx4^+$ cells in tissue cryosections, 10 microscopic fields (20×) from three WT and Cbx4KO skin sections were included in the analysis. For quantification of $Ki67^+$, Ivl^+, and $Nefl^+$ cells cultured in vitro, five microscopic fields (20×) taken from the center and each of the four sides of the well were used in the analysis. Data were pooled, the means ± SD were calculated, and statistical analysis was performed using a two-tailed *t* test ($\alpha = 0.05$).

Immunofluorescence intensity was determined using ImageJ software as described previously (McCloy et al., 2014). In brief, red or green fluorescent signals were collected from experimental tissues in RGB format using the same exposure conditions. To measure the fluorescence intensity at each pixel, the RGB images were converted to 8-bit grayscale format. Regions of interest of distinct size were selected within WT or Cbx4KO epidermis and dermis, and the corrected values of total cell fluorescence were calculated for each selected area using the following formula: corrected total cell fluorescence = integrated density − (area of selected cell × mean fluorescence of background readings). For pairwise comparisons, a two-tailed *t* test ($\alpha = 0.05$) was used. Where multiple samples were compared, a one-way analysis of variance (ANOVA) was used, followed by the Newman–Keuls test ($\alpha = 0.05$).

ChIP-seq and ChIP-qPCR assays

ChIP was performed using epidermal KCs isolated from newborn mouse skin and anti-H3K27me3, anti-Cbx4, and anti-H2AK119ub1 antibodies (Table S5). In brief, a single-cell suspension of mouse epidermal KCs was prepared after overnight digestion in 5 mg/ml dispase (Roche) at 4°C, followed by a 5-min treatment with 0.2% trypsin (Life Technologies). Basal epidermal KCs were sorted by FACS and further processed using a ChIP-IT High Sensitivity kit (Active Motive). 5×10^6 PFA-fixed cells were used as a starting material. Indexed ChIP-seq libraries were generated using NEBNext reagents (New England Biolabs, Inc.), and ChIP libraries were sequenced on the HiSeq 2500 platform (Illumina), producing 30–70 million reads per library. Sequencing reads were aligned to the mm9 mouse genome assembly (University of California, Santa Cruz, Genome Browser). Specific areas of binding were identified with Sicer using default settings. For ChIP-qPCR, precipitated DNA was analyzed using primers designed for the promoter regions of *Cbx4*, *Lor*, *Nefl*, and *Cdkn2a* genes (Table S3). ChIP-qPCR data were pooled, means ± SD were calculated, and statistical analysis was performed using a one-way ANOVA test as described previously (Mardaryev et al., 2011).

Embryonic tissue culture

Whole dorsal skin culture from E13.5 $p63^{+/-}$ embryos were prepared and maintained as previously described (Botchkarev et al., 1999). In brief, skin samples were dissected from embryos and cultured in the 6-well plates containing Williams' medium E. Within 2 h after the cul-

Published December 28, 2015

ture preparation, tissue samples were infected with p63 shRNA lentivirus in combination with either Cbx4-expressing or control lentiviruses and the addition of 10 µg/ml polybrene (Sigma-Aldrich) for 48 h. The tissue was frozen and embedded into optimal cutting temperature medium for subsequent immunofluorescent and qRT-PCR analyses.

Online supplemental material

Fig. S1 shows expression of the PRC1/PRC2 and *Nefl* genes in mouse epidermis during development. Fig. S2 shows characterization of the changes in gene expression in the epidermis of Cbx4KO mice and in primary KCs after Cbx4 knockdown. Fig. S3 shows analyses of the senescence and apoptotic markers in WT and Cbx4-deficient skin. Fig. S4 shows the details of the epidermal and Merkel cell differentiation in Cbx4KO and WT mice. Table S1 shows expression of the PRC1 and PRC2 genes in epidermal KCs at different stages of epidermal development. Table S2 shows Cbx4 target genes up-regulated in the skin epithelium of p63KO mice. Tables S3 and S4 present a list of primers used for qRT-PCR analyses and a list of antibodies used in this study, respectively. Table S5 shows Cbx4 target genes in epidermal KCs. Online supplemental material is available at http://www.jcb.org/cgi/content/full/jcb.201506065/DC1.

Acknowledgments

This work was supported by grants from the Biotechnology and Biological Sciences Research Council (BB/K010050/1), the Medical Research Council (MRC; MR/M010015/1), the National Institute of Arthritis and Musculoskeletal and Skin Diseases (AR049778 and AR064580), and EpiGeneSys to V.A. Botchkarev; from MRC (G1000846) to C.A. Jahoda; from the European Research Council, the Association for International Cancer Research, the Foundation La Marató, the Spanish Ministry of Economy and Development, the Foundation Vencer el Cancer, the Government of Cataluña (SGR and Mario Salviá), the Foundation Botín, and the Institute for Research in Biomedicine Barcelona to S.A. Benitah; and from the National Science Foundation of China (81461138034) to G.-L. Xu.

The authors declare no competing financial interests.

Submitted: 14 June 2015
Accepted: 17 November 2015

References

Ahmed, M.I., A.N. Mardaryev, C.J. Lewis, A.A. Sharov, and N.V. Botchkareva. 2011. MicroRNA-21 is an important downstream component of BMP signalling in epidermal keratinocytes. *J. Cell Sci.* 124:3399–3404. http://dx.doi.org/10.1242/jcs.086710

Ahmed, M.I., M. Alam, V.U. Emelianov, K. Poterlowicz, A. Patel, A.A. Sharov, A.N. Mardaryev, and N.V. Botchkareva. 2014. MicroRNA-214 controls skin and hair follicle development by modulating the activity of the Wnt pathway. *J. Cell Biol.* 207:549–567. http://dx.doi.org/10.1083/jcb.201404001

Bardot, E.S., V.J. Valdes, J. Zhang, C.N. Perdigoto, S. Nicolis, S.A. Hearn, J.M. Silva, and E. Ezhkova. 2013. Polycomb subunits Ezh1 and Ezh2 regulate the Merkel cell differentiation program in skin stem cells. *EMBO J.* 32:1990–2000. http://dx.doi.org/10.1038/emboj.2013.110

Benitah, S.A., and M. Frye. 2012. Stem cells in ectodermal development. *J. Mol. Med.* 90:783–790. http://dx.doi.org/10.1007/s00109-012-0908-x

Blackledge, N.P., A.M. Farcas, T. Kondo, H.W. King, J.F. McGouran, L.L. Hanssen, S. Ito, S. Cooper, K. Kondo, Y. Koseki, et al. 2014. Variant PRC1 complex-dependent H2A ubiquitylation drives PRC2 recruitment and polycomb domain formation. *Cell.* 157:1445–1459. http://dx.doi.org/10.1016/j.cell.2014.05.004

Blanpain, C., and E. Fuchs. 2009. Epidermal homeostasis: A balancing act of stem cells in the skin. *Nat. Rev. Mol. Cell Biol.* 10:207–217. http://dx.doi.org/10.1038/nrm2636

Blanpain, C., and E. Fuchs. 2014. Stem cell plasticity. Plasticity of epithelial stem cells in tissue regeneration. *Science.* 344:1242281. http://dx.doi.org/10.1126/science.1242281

Botchkarev, V.A., and E.R. Flores. 2014. p53/p63/p73 in the epidermis in health and disease. *Cold Spring Harb. Perspect. Med.* 4:301–312. http://dx.doi.org/10.1101/cshperspect.a015248

Botchkarev, V.A., E.M. Peters, N.V. Botchkareva, M. Maurer, and R. Paus. 1999. Hair cycle-dependent changes in adrenergic skin innervation, and hair growth modulation by adrenergic drugs. *J. Invest. Dermatol.* 113:878–887. http://dx.doi.org/10.1046/j.1523-1747.1999.00791.x

Botchkarev, V.A., M.R. Gdula, A.N. Mardaryev, A.A. Sharov, and M.Y. Fessing. 2012. Epigenetic regulation of gene expression in keratinocytes. *J. Invest. Dermatol.* 132:2505–2521. http://dx.doi.org/10.1038/jid.2012.182

Botchkareva, N.V., V.A. Botchkarev, L.H. Chen, G. Lindner, and R. Paus. 1999. A role for p75 neurotrophin receptor in the control of hair follicle morphogenesis. *Dev. Biol.* 216:135–153. http://dx.doi.org/10.1006/dbio.1999.9464

Botchkareva, N.V., V.A. Botchkarev, P. Welker, M. Airaksinen, W. Roth, P. Suvanto, S. Müller-Röver, I.M. Hadshiew, C. Peters, and R. Paus. 2000. New roles for glial cell line-derived neurotrophic factor and neurturin: Involvement in hair cycle control. *Am. J. Pathol.* 156:1041–1053. http://dx.doi.org/10.1016/S0002-9440(10)64972-3

Cheutin, T., and G. Cavalli. 2014. Polycomb silencing: From linear chromatin domains to 3D chromosome folding. *Curr. Opin. Genet. Dev.* 25:30–37. http://dx.doi.org/10.1016/j.gde.2013.11.016

Cooper, S., M. Dienstbier, R. Hassan, L. Schermelleh, J. Sharif, N.P. Blackledge, V. De Marco, S. Elderkin, H. Koseki, R. Klose, et al. 2014. Targeting polycomb to pericentric heterochromatin in embryonic stem cells reveals a role for H2AK119u1 in PRC2 recruitment. *Cell Reports.* 7:1456–1470. http://dx.doi.org/10.1016/j.celrep.2014.04.012

De Rosa, L., D. Antonini, G. Ferone, M.T. Russo, P.B. Yu, R. Han, and C. Missero. 2009. p63 Suppresses non-epidermal lineage markers in a bone morphogenetic protein-dependent manner via repression of Smad7. *J. Biol. Chem.* 284:30574–30582. http://dx.doi.org/10.1074/jbc.M109.049619

Ezhkova, E., H.A. Pasolli, J.S. Parker, N. Stokes, I.H. Su, G. Hannon, A. Tarakhovsky, and E. Fuchs. 2009. Ezh2 orchestrates gene expression for the stepwise differentiation of tissue-specific stem cells. *Cell.* 136:1122–1135. http://dx.doi.org/10.1016/j.cell.2008.12.043

Ezhkova, E., W.H. Lien, N. Stokes, H.A. Pasolli, J.M. Silva, and E. Fuchs. 2011. EZH1 and EZH2 cogovern histone H3K27 trimethylation and are essential for hair follicle homeostasis and wound repair. *Genes Dev.* 25:485–498. http://dx.doi.org/10.1101/gad.2019811

Fessing, M.Y., A.N. Mardaryev, M.R. Gdula, A.A. Sharov, T.Y. Sharova, V. Rapisarda, K.B. Gordon, A.D. Smorodchenko, K. Poterlowicz, G. Ferone, et al. 2011. p63 regulates Satb1 to control tissue-specific chromatin remodeling during development of the epidermis. *J. Cell Biol.* 194:825–839. http://dx.doi.org/10.1083/jcb.201101148

Frye, M., and S.A. Benitah. 2012. Chromatin regulators in mammalian epidermis. *Semin. Cell Dev. Biol.* 23:897–905. http://dx.doi.org/10.1016/j.semcdb.2012.08.009

Fuchs, E. 2007. Scratching the surface of skin development. *Nature.* 445:834–842. http://dx.doi.org/10.1038/nature05659

Grillo, G., F. Licciulli, S. Liuni, E. Sbisà, and G. Pesole. 2003. PatSearch: A program for the detection of patterns and structural motifs in nucleotide sequences. *Nucleic Acids Res.* 31:3608–3612. http://dx.doi.org/10.1093/nar/gkg548

Hobert, O., and H. Westphal. 2000. Functions of LIM-homeobox genes. *Trends Genet.* 16:75–83. http://dx.doi.org/10.1016/S0168-9525(99)01883-1

Hunt, D.P., C. Jahoda, and S. Chandran. 2009. Multipotent skin-derived precursors: From biology to clinical translation. *Curr. Opin. Biotechnol.* 20:522–530. http://dx.doi.org/10.1016/j.copbio.2009.10.004

Jensen, K.B., R.R. Driskell, and F.M. Watt. 2010. Assaying proliferation and differentiation capacity of stem cells using disaggregated adult mouse epidermis. *Nat. Protoc.* 5:898–911.

Jordanova, A., P. De Jonghe, C.F. Boerkoel, H. Takashima, E. De Vriendt, C. Ceuterick, J.J. Martin, I.J. Butler, P. Mancias, S.Ch. Papasozomenos, et al. 2003. Mutations in the neurofilament light chain gene (NEFL) cause early onset severe Charcot-Marie-Tooth disease. *Brain.* 126:590–597. http://dx.doi.org/10.1093/brain/awg059

Kalb, R., S. Latwiel, H.I. Baymaz, P.W. Jansen, C.W. Müller, M. Vermeulen, and J. Müller. 2014. Histone H2A monoubiquitination promotes histone H3 methylation in Polycomb repression. *Nat. Struct. Mol. Biol.* 21:569–571. http://dx.doi.org/10.1038/nsmb.2833

Keyes, W.M., M. Pecoraro, V. Aranda, E. Vernersson-Lindahl, W. Li, H. Vogel, X. Guo, E.L. Garcia, T.V. Michurina, G. Enikolopov, et al. 2011. ΔNp63α is an oncogene that targets chromatin remodeler Lsh to drive skin stem cell proliferation and tumorigenesis. *Cell Stem Cell.* 8:164–176. http://dx.doi.org/10.1016/j.stem.2010.12.009

Khavari, D.A., G.L. Sen, and J.L. Rinn. 2010. DNA methylation and epigenetic control of cellular differentiation. *Cell Cycle.* 9:3880–3883. http://dx.doi.org/10.4161/cc.9.19.13385

Koster, M.I., and D.R. Roop. 2007. Mechanisms regulating epithelial stratification. *Annu. Rev. Cell Dev. Biol.* 23:93–113. http://dx.doi.org/10.1146/annurev.cellbio.23.090506.123357

Kouwenhoven, E.N., H. van Bokhoven, and H. Zhou. 2015. Gene regulatory mechanisms orchestrated by p63 in epithelial development and related disorders. *Biochim. Biophys. Acta.* 1849:590–600.

LeBoeuf, M., A. Terrell, S. Trivedi, S. Sinha, J.A. Epstein, E.N. Olson, E.E. Morrisey, and S.E. Millar. 2010. Hdac1 and Hdac2 act redundantly to control p63 and p53 functions in epidermal progenitor cells. *Dev. Cell.* 19:807–818. http://dx.doi.org/10.1016/j.devcel.2010.10.015

Li, B., J. Zhou, P. Liu, J. Hu, H. Jin, Y. Shimono, M. Takahashi, and G. Xu. 2007. Polycomb protein Cbx4 promotes SUMO modification of de novo DNA methyltransferase Dnmt3a. *Biochem. J.* 405:369–378. http://dx.doi.org/10.1042/BJ20061873

Liu, B., Y.F. Liu, Y.R. Du, A.N. Mardaryev, W. Yang, H. Chen, Z.M. Xu, C.Q. Xu, X.R. Zhang, V.A. Botchkarev, et al. 2013. Cbx4 regulates the proliferation of thymic epithelial cells and thymus function. *Development.* 140:780–788. http://dx.doi.org/10.1242/dev.085035

Luis, N.M., L. Morey, S. Mejetta, G. Pascual, P. Janich, B. Kuebler, L. Cozutto, G. Roma, E. Nascimento, M. Frye, et al.. 2011. Regulation of human epidermal stem cell proliferation and senescence requires polycomb-dependent and -independent functions of Cbx4. *Cell Stem Cell.* 9:233–246. http://dx.doi.org/10.1016/j.stem.2011.07.013

Mardaryev, A.N., N. Meier, K. Poterlowicz, A.A. Sharov, T.Y. Sharova, M.I. Ahmed, V. Rapisarda, C. Lewis, M.Y. Fessing, T.M. Ruenger, et al. 2011. Lhx2 differentially regulates Sox9, Tcf4 and Lgr5 in hair follicle stem cells to promote epidermal regeneration after injury. *Development.* 138:4843–4852. http://dx.doi.org/10.1242/dev.070284

Mardaryev, A.N., M.R. Gdula, J.L. Yarker, V.U. Emelianov, K. Poterlowicz, A.A. Sharov, T.Y. Sharova, J.A. Scarpa, B. Joffe, I. Solovei, et al. 2014. p63 and Brg1 control developmentally regulated higher-order chromatin remodelling at the epidermal differentiation complex locus in epidermal progenitor cells. *Development.* 141:101–111. http://dx.doi.org/10.1242/dev.103200

McCloy, R.A., S. Rogers, C.E. Caldon, T. Lorca, A. Castro, and A. Burgess. 2014. Partial inhibition of Cdk1 in G_2 phase overrides the SAC and decouples mitotic events. *Cell Cycle.* 13:1400–1412. http://dx.doi.org/10.4161/cc.28401

Mejetta, S., L. Morey, G. Pascual, B. Kuebler, M.R. Mysliwiec, Y. Lee, R. Shiekhattar, L. Di Croce, and S.A. Benitah. 2011. Jarid2 regulates mouse epidermal stem cell activation and differentiation. *EMBO J.* 30:3635–3646. http://dx.doi.org/10.1038/emboj.2011.265

Merrill, J.C., T.A. Melhuish, M.H. Kagey, S.H. Yang, A.D. Sharrocks, and D. Wotton. 2010. A role for non-covalent SUMO interaction motifs in Pc2/CBX4 E3 activity. *PLoS One.* 5:e8794. http://dx.doi.org/10.1371/journal.pone.0008794

Mills, A.A., B. Zheng, X.J. Wang, H. Vogel, D.R. Roop, and A. Bradley. 1999. *p63* is a *p53* homologue required for limb and epidermal morphogenesis. *Nature.* 398:708–713. http://dx.doi.org/10.1038/19531

Mitew, S., C.M. Hay, H. Peckham, J. Xiao, M. Koenning, and B. Emery. 2014. Mechanisms regulating the development of oligodendrocytes and central nervous system myelin. *Neuroscience.* 276:29–47. http://dx.doi.org/10.1016/j.neuroscience.2013.11.029

Montague, P., P.J. Dickinson, A.S. McCallion, G.J. Stewart, A. Savioz, R.W. Davies, P.G. Kennedy, and I.R. Griffiths. 1997. Developmental expression of the murine *Mobp* gene. *J. Neurosci. Res.* 49:133–143. http://dx.doi.org/10.1002/(SICI)1097-4547(19970715)49:2<133::AID-JNR2>3.0.CO;2-A

Morey, L., G. Pascual, L. Cozzuto, G. Roma, A. Wutz, S.A. Benitah, and L. Di Croce. 2012. Nonoverlapping functions of the Polycomb group Cbx family of proteins in embryonic stem cells. *Cell Stem Cell.* 10:47–62. http://dx.doi.org/10.1016/j.stem.2011.12.006

Mostoslavsky, G., D.N. Kotton, A.J. Fabian, J.T. Gray, J.S. Lee, and R.C. Mulligan. 2005. Efficiency of transduction of highly purified murine hematopoietic stem cells by lentiviral and oncoretroviral vectors under conditions of minimal *in vitro* manipulation. *Mol. Ther.* 11:932–940. http://dx.doi.org/10.1016/j.ymthe.2005.01.005

Patthey, C., and L. Gunhaga. 2011. Specification and regionalisation of the neural plate border. *Eur. J. Neurosci.* 34:1516–1528. http://dx.doi.org/10.1111/j.1460-9568.2011.07871.x

Pelling, M., N. Anthwal, D. McNay, G. Gradwohl, A.B. Leiter, F. Guillemot, and S.L. Ang. 2011. Differential requirements for neurogenin 3 in the development of POMC and NPY neurons in the hypothalamus. *Dev. Biol.* 349:406–416. http://dx.doi.org/10.1016/j.ydbio.2010.11.007

Perdigoto, C.N., V.J. Valdes, E.S. Bardot, and E. Ezhkova. 2014. Epigenetic regulation of epidermal differentiation. *Cold Spring Harb. Perspect. Med.* 4:281–300. http://dx.doi.org/10.1101/cshperspect.a015263

Schwartz, Y.B., and V. Pirrotta. 2014. Ruled by ubiquitylation: A new order for polycomb recruitment. *Cell Reports.* 8:321–325. http://dx.doi.org/10.1016/j.celrep.2014.07.001

Sen, G.L., D.E. Webster, D.I. Barragan, H.Y. Chang, and P.A. Khavari. 2008. Control of differentiation in a self-renewing mammalian tissue by the histone demethylase JMJD3. *Genes Dev.* 22:1865–1870. http://dx.doi.org/10.1101/gad.1673508

Sen, G.L., J.A. Reuter, D.E. Webster, L. Zhu, and P.A. Khavari. 2010. DNMT1 maintains progenitor function in self-renewing somatic tissue. *Nature.* 463:563–567. http://dx.doi.org/10.1038/nature08683

Sharov, A.A., G.Z. Li, T.N. Palkina, T.Y. Sharova, B.A. Gilchrest, and V.A. Botchkarev. 2003. Fas and c-kit are involved in the control of hair follicle melanocyte apoptosis and migration in chemotherapy-induced hair loss. *J. Invest. Dermatol.* 120:27–35. http://dx.doi.org/10.1046/j.1523-1747.2003.12022.x

Sharov, A.A., M. Fessing, R. Atoyan, T.Y. Sharova, C. Haskell-Luevano, L. Weiner, K. Funa, J.L. Brissette, B.A. Gilchrest, and V.A. Botchkarev. 2005. Bone morphogenetic protein (BMP) signaling controls hair pigmentation by means of cross-talk with the melanocortin receptor-1 pathway. *Proc. Natl. Acad. Sci. USA.* 102:93–98. http://dx.doi.org/10.1073/pnas.0408455102

Sharov, A.A., T.Y. Sharova, A.N. Mardaryev, A. Tommasi di Vignano, R. Atoyan, L. Weiner, S. Yang, J.L. Brissette, G.P. Dotto, and V.A. Botchkarev. 2006. Bone morphogenetic protein signaling regulates the size of hair follicles and modulates the expression of cell cycle-associated genes. *Proc. Natl. Acad. Sci. USA.* 103:18166–18171. http://dx.doi.org/10.1073/pnas.0608899103

Sharov, A.A., A.N. Mardaryev, T.Y. Sharova, M. Grachtchouk, R. Atoyan, H.R. Byers, J.T. Seykora, P. Overbeek, A. Dlugosz, and V.A. Botchkarev. 2009. Bone morphogenetic protein antagonist noggin promotes skin tumorigenesis via stimulation of the Wnt and Shh signaling pathways. *Am. J. Pathol.* 175:1303–1314. http://dx.doi.org/10.2353/ajpath.2009.090163

Sher, F., R. Rössler, N. Brouwer, V. Balasubramaniyan, E. Boddeke, and S. Copray. 2008. Differentiation of neural stem cells into oligodendrocytes: Involvement of the polycomb group protein Ezh2. *Stem Cells.* 26:2875–2883. http://dx.doi.org/10.1634/stemcells.2008-0121

Sher, F., E. Boddeke, M. Olah, and S. Copray. 2012. Dynamic changes in Ezh2 gene occupancy underlie its involvement in neural stem cell self-renewal and differentiation towards oligodendrocytes. *PLoS One.* 7:e40399. http://dx.doi.org/10.1371/journal.pone.0040399

Simon, J.A., and R.E. Kingston. 2013. Occupying chromatin: Polycomb mechanisms for getting to genomic targets, stopping transcriptional traffic, and staying put. *Mol. Cell.* 49:808–824. http://dx.doi.org/10.1016/j.molcel.2013.02.013

Slack, J.M. 2008. Origin of stem cells in organogenesis. *Science.* 322:1498–1501. http://dx.doi.org/10.1126/science.1162782

Turinetto, V., and C. Giachino. 2015. Multiple facets of histone variant H2AX: A DNA double-strand-break marker with several biological functions. *Nucleic Acids Res.* 43:2489–2498. http://dx.doi.org/10.1093/nar/gkv061

Vanbokhoven, H., G. Melino, E. Candi, and W. Declercq. 2011. p63, a story of mice and men. *J. Invest. Dermatol.* 131:1196–1207. http://dx.doi.org/10.1038/jid.2011.84

Van Keymeulen, A., G. Mascre, K.K. Youseff, I. Harel, C. Michaux, N. De Geest, C. Szpalski, Y. Achouri, W. Bloch, B.A. Hassan, and C. Blanpain. 2009. Epidermal progenitors give rise to Merkel cells during embryonic development and adult homeostasis. *J. Cell Biol.* 187:91–100. http://dx.doi.org/10.1083/jcb.200907080

Viganò, M.A., and R. Mantovani. 2007. Hitting the numbers: The emerging network of p63 targets. *Cell Cycle.* 6:233–239. http://dx.doi.org/10.4161/cc.6.3.3802

Wallén, A., and T. Perlmann. 2003. Transcriptional control of dopamine neuron development. *Ann. N. Y. Acad. Sci.* 991:48–60. http://dx.doi.org/10.1111/j.1749-6632.2003.tb07462.x

Yang, A., R. Schweitzer, D. Sun, M. Kaghad, N. Walker, R.T. Bronson, C. Tabin, A. Sharpe, D. Caput, C. Crum, and F. McKeon. 1999. p63 is essential for regenerative proliferation in limb, craniofacial and epithelial development. *Nature.* 398:714–718. http://dx.doi.org/10.1038/19539

Table S5. **Cbx4-dependent Polycomb targets in mouse epidermal progenitor cells**

Gene name	Description	CBX4KO versus WT	Cbx4 ChIP-seq peak start	Cbx4 ChIP-seq peak end	H3K27me3 ChIP-seq peak start	H3K27me3 ChIP-seq peak end
Abca8b	ATP-binding cassette, sub-family A (ABC1), member 8b (Abca8b) [NM_013851]	6.7	109891303	109892702	109892065	109893060
Abcb4	ATP-binding cassette, sub-family B (MDR/TAP), member 4 (Abcb4) [NM_008830]	166.7	8861441	8862016	8893021	8894618
Ablim1	actin-binding LIM protein 1	3.8	57377643	57378322	57396863	57400086
Acaa2	acetyl-Coenzyme A acyltransferase 2 (mitochondrial 3-oxoacyl-Coenzyme A thiolase) (Acaa2), nuclear gene encoding mitochondrial protein [NM_177470]	4.1	74965315	74965865	74958473	74960177
Acacb	acetyl-Coenzyme A carboxylase beta (Acacb) [NM_133904]	2.2	114614986	114615883	114595162	114596740
Accn1	amiloride-sensitive cation channel 1, neuronal (degenerin) (Accn1), transcript variant MDEG2 [NM_007384]	4.9	81757576	81758271	81779017	81782808
Acot12	acyl-CoA thioesterase 12 (Acot12) [NM_028790]	6.7	91877528	91878424	91880131	91881976
Actr3b	ARP3 actin-related protein 3B	12.7	25274562	25275337	25319588	25321790
Adam1b	a disintegrin and metallopeptidase domain 1b (Adam1b) [NM_172125]	2.2	121943925	121945418	121952680	121954960
Adam23	a disintegrin and metallopeptidase domain 23 (Adam23), [NM_011780]	26.8	63504710	63505387	63491467	63493602
Adar	adenosine deaminase, RNA-specific (Adar), [NM_001038587]	2.1	89428375	89429316	89538275	89541141
Adck1	aarF domain containing kinase 1	4	89609890	89611017	89619351	89620799
Adck3	aarF domain containing kinase 3 (Adck3), nuclear gene encoding mitochondrial protein, [NM_023341]	59.7	182144228	182145215	182144274	182147470
Adcy1	adenylate cyclase 1 (Adcy1) [NM_009622]	6.1	7001305	7002626	6962317	6969103
Adcy5	adenylate cyclase 5 (Adcy5) [NM_001012765]	8.3	35093984	35094713	35152404	35162296
Adora2a	adenosine A2a receptor (Adora2a) [NM_009630]	3	74811436	74812183	74766682	74768072
Adra1a	adrenergic receptor, alpha 1a (Adra1a) [NM_013461]	4.7	67326057	67326796	67253722	67257789
Agap2	ArfGAP with GTPase domain, ankyrin repeat and PH domain 2 (Agap2) [NM_001033263]	248.9	126511962	126513078	126511826	126523218
Agtr1a	angiotensin II receptor, type 1a (Agtr1a) [NM_177322]	37.7	30431640	30432259	30426387	30427318
Agxt2l1	alanine-glyoxylate aminotransferase 2–like 1 (Agxt2l1), [NM_027907]	2.8	130240502	130241157	130319828	130321096
Ajap1	adherens junction associated protein 1 (Ajap1) [NM_001099299]	236.6	152828273	152829100	152860367	152864210
Aldh1a3	aldehyde dehydrogenase family 1, subfamily A3 (Aldh1a3) [NM_053080]	11.1	73659237	73659977	73571152	73574988
Alk	anaplastic lymphoma kinase	3.7	73011067	73011737	72951844	72954641
Ambra1	autophagy/beclin 1 regulator 1 (Ambra1), [NM_172669]	2.5	91612175	91613104	91612325	91614178
Amfr	autocrine motility factor receptor (Amfr) [NM_011787]	4.4	96547791	96548361	96496004	96499340
Amz1	archaelysin family metallopeptidase 1 (Amz1) [NM_173405]	7.1	141234507	141237202	141218947	141221387
Ank1	ankyrin 1, erythroid (Ank1), [NM_031158]	4.5	24114223	24115251	24087878	24089725
Ank3	ankyrin 3, epithelial (Ank3), [NM_146005]	11.2	69074432	69075199	68961340	68962442
Ankrd13a	ankyrin repeat domain 13a (Ankrd13a) [NM_026718]	2.3	115206985	115208253	115211903	115213547
Ankrd44	ankyrin repeat domain 44	3.7	54995259	54995957	54924791	54925936
Anp32a	acidic (leucine-rich) nuclear phosphoprotein 32 family, member A (Anp32a) [NM_009672]	2.5	62163331	62164009	62194574	62198289
Antxr1	anthrax toxin receptor 1 (Antxr1) [NM_054041]	3.5	87277754	87278579	87276656	87279278
Anxa3	annexin A3 (Anxa3) [NM_013470]	2.2	97241590	97242268	97196666	97197675
Aox1	aldehyde oxidase 1 (Aox1) [NM_009676]	34	58081166	58081703	58111530	58112869
Ap2s1	adaptor-related protein complex 2, sigma 1 subunit (Ap2s1) [NM_198613]	3.5	17332099	17334982	17325884	17331369
Ap3b2	adaptor-related protein complex 3, beta 2 subunit (Ap3b2) [NM_021492]	488.9	88639909	88641241	88628780	88630699
Ap3d1	adaptor-related protein complex 3, delta 1 subunit (Ap3d1) [NM_007460]	247.7	80195050	80196513	80189143	80194171
Apob	apolipoprotein B (Apob) [NM_009693]	4.7	7994867	7995900	8068552	8069828
Apol8	apolipoprotein L 8	85.1	77582741	77584070	77582767	77584858
Aqp12	aquaporin 12 (Aqp12), [NM_177587]	5.4	94930097	94932003	94927326	94934262
Arf1	ADP-ribosylation factor 1 (Arf1), [NM_007476]	2.2	59065665	59066434	59050447	59059539
Arhgap20	Rho GTPase activating protein 20 (Arhgap20) [NM_175535]	66.1	51504719	51505324	51572515	51575490
Arhgef7	Rho guanine nucleotide exchange factor (GEF7) (Arhgef7), [NM_001113517]	9.9	11746678	11748148	11729934	11731640
Arx	aristaless related homeobox (Arx) [NM_007492]	3.3	90629174	90629640	90530192	90536461
Atf1	activating transcription factor 1 (Atf1) [NM_007497]	2	100009921	100011245	100012144	100013726
Atp12a	ATPase, H/K transporting, nongastric, alpha	177.1	56948986	56949621	56967874	56969530

	polypeptide (Atp12a) [NM_138652]					
Atp1a2	ATPase, Na/K transporting, alpha 2 polypeptide (Atp1a2) [NM_178405]	31.7	174215183	174216559	174228984	174232036
Atp2b1	ATPase, Ca^{+} transporting, plasma membrane 1 (Atp2b1) [NM_026482]	2.2	98464762	98465396	98199991	98201125
AW554918	expressed sequence AW554918 (AW554918) [NM_001033532]	2.4	25276175	25276980	25177026	25177956
B230206H07Rik	RIKEN cDNA B230206H07 gene (B230206H07Rik), non-coding RNA [NR_033532]	25.4	148540503	148542216	148540344	148544615
B3gat2	beta-1,3-glucuronyltransferase 2 (glucuronosyltransferase S) (B3gat2) [NM_172124]	5.3	23773502	23774309	23767388	23771402
BC018507	cDNA sequence BC018507 (BC018507) [NM_144837]	4.2	70686081	70686844	70741015	70745284
BC051665	cDNA sequence BC051665 (BC051665) [NM_199148]	21.4	60853246	60854165	60861555	60863611
Brap	BRCA1-associated protein (Brap) [NM_028227]	2.3	122116137	122116861	122126705	122127577
Brms1l	breast cancer metastasis-suppressor 1-like (Brms1l) [NM_001037756]	5.5	56941393	56941929	56961074	56962599
Bves	blood vessel epicardial substance (Bves) [NM_024285]	7.1	45071163	45072319	45054060	45056212
C030034L19Rik	RIKEN cDNA C030034L19 gene	3.3	9450459	9451109	9431918	9433424
C130022K22Rik	RIKEN cDNA C130022K22 gene (C130022K22Rik) [NM_172730]	2.8	91815338	91816125	91812562	91816568
C1ql2	complement component 1, q subcomponent–like 2 (C1ql2) [NM_207233]	3.8	122278908	122279671	122234088	122240580
C1qtnf9	C1q and tumor necrosis factor–related protein 9 (C1qtnf9) [NM_183175]	11.1	61379361	61381649	61383482	61386250
C2cd4b	C2 calcium-dependent domain containing 4B (C2cd4b) [NM_001081314]	24.1	67517459	67518828	67606625	67609182
C8b	complement component 8, beta polypeptide (C8b) [NM_133882]	28.4	104445025	104445790	104433442	104434707
Cacng1	calcium channel, voltage-dependent, gamma subunit 1 (Cacng1) [NM_007582]	3.4	107585222	107586059	107564348	107568533
Cacng8	calcium channel, voltage-dependent, gamma subunit 8 (Cacng8) [NM_133190]	12.2	3368691	3369298	3364555	3367964
Calcr	calcitonin receptor (Calcr), b [NM_007588]	9.4	3713254	3714814	3713068	3714926
Cartpt	CART prepropeptide (Cartpt), [NM_013732]	2.1	100715390	100716040	100668533	100671536
Casc1	cancer susceptibility candidate 1	2.8	145144930	145145695	145153407	145154461
Cbr4	carbonyl reductase 4 (Cbr4) [NM_145595]	5.7	64043033	64043783	63937548	63940073
Ccbe1	collagen and calcium binding EGF domains 1 (Ccbe1) [NM_178793]	2.1	66523434	66524483	66502971	66503954
Ccdc90a	coiled-coil domain containing 90A (Ccdc90a) [NM_001081059]	56.1	43644896	43645907	43666384	43668002
Cd93	CD93 antigen (Cd93) [NM_010740]	4.1	148275308	148275952	148266593	148269840
Cdc7	cell division cycle 7 (*S. cerevisiae*) (Cdc7) [NM_009863]	2.3	107484048	107484897	107431942	107433569
Cdca7l	cell division cycle–associated 7 like (Cdca7l) [NM_146040]	10.6	118974676	118975352	119008545	119010548
Cdh4	cadherin 4 (Cdh4) [NM_009867]	4.2	179203401	179205682	179174839	179180146
Cdkal1	CDK5 regulatory subunit associated protein 1–like 1 (Cdkal1) [NM_144536]	4.4	29925470	29926121	29794265	29795233
Cdon	cell adhesion molecule-related/down-regulated by oncogenes (Cdon) [NM_021339]	3.3	35216184	35216898	35220568	35221663
Cdyl2	chromodomain protein, Y chromosome–like 2 (Cdyl2) [NM_029441]	3.3	119262013	119262804	119173633	119175303
Ceacam19	carcinoembryonic antigen-related cell adhesion molecule 19 (Ceacam19) [NM_177036]	6.5	20462795	20464540	20461980	20464753
Cenpf	centromere protein F (Cenpf) [NM_001081363]	2.2	191509464	191510229	191503124	191504092
Cfi	complement component factor i (Cfi) [NM_007686]	160.6	129552535	129553190	129550224	129551018
Chgb	chromogranin B (Chgb) [NM_007694]	5.2	132590732	132591513	132606618	132608242
Chmp2b	charged multivesicular body protein 2B (Chmp2b) [NM_026879]	2.1	65544952	65545623	65571578	65573518
Chordc1	cysteine and histidine-rich domain (CHORD)-containing, zinc-binding protein 1 (Chordc1) [NM_025844]	6.4	18104353	18105271	18061695	18062878
Chst12	carbohydrate sulfotransferase 12 (Chst12) [NM_021528]	3.1	140964970	140966161	140968380	140970431
Ckmt2	creatine kinase, mitochondrial 2 (Ckmt2), nuclear gene encoding mitochondrial protein [NM_198415]	227.5	92028986	92030308	92048170	92050072
Clec16a	C-type lectin domain family 16, member A (Clec16a), [NM_177562]	5.9	10609925	10611544	10609803	10611867
Clic6	chloride intracellular channel 6 (Clic6), nuclear gene encoding mitochondrial protein [NM_172469]	2.6	92524818	92526178	92497451	92500215
Cln8	ceroid-lipofuscinosis, neuronal 8 (Cln8) [NM_012000]	3.6	14838933	14840129	14839039	14840931
Clybl	citrate lyase beta like (Clybl) [NM_029556]	24.8	122632308	122633329	122570818	122572191
Cnksr3	Cnksr family member 3 (Cnksr3) [NM_172546]	6.6	3082532	3083144	3150511	3151976
Cnr1	cannabinoid receptor 1 (brain) (Cnr1) [NM_007726]	2.3	34030786	34032028	33994635	33995767
Cntn3	contactin 3 (Cntn3) [NM_008779]	2.4	102347283	102347929	102513536	102514888
Cog2	component of oligomeric Golgi complex 2 (Cog2)	2.9	127022129	127022902	127034487	127035569

	[NM_029746]					
Cog6	component of oligomeric Golgi complex 6 (Cog6) [NM_026225]	2.9	52756565	52757205	52802557	52803626
Cog7	component of oligomeric Golgi complex 7 (Cog7) [NM_001033318]	2.8	129094610	129095548	129143257	129144577
Col13a1	collagen, type XIII, alpha 1 (Col13a1) [NM_007731]	12	61418621	61420135	61435861	61443604
Col14a1	collagen, type XIV, alpha 1 (Col14a1) [NM_181277]	20.1	55185084	55185863	55137772	55141026
Corin	corin (Corin), [NM_016869]	25.1	72911176	72911830	72893988	72896415
Cpn2	carboxypeptidase N, polypeptide 2 (Cpn2) [NM_027904]	137.6	30265239	30266075	30256568	30261523
Cryz	crystallin, zeta (Cryz) [NM_009968]	4.9	154243017	154243626	154210360	154211601
Ctdp1	CTD (C-terminal domain, RNA polymerase II, polypeptide A) phosphatase, subunit 1 (Ctdp1) [NM_026295]	25	80673132	80674222	80687731	80689822
Ctnnd2	catenin (cadherin-associated protein), delta 2 (Ctnnd2) [NM_008729]	6.2	30143203	30144130	30101375	30104103
Cttn	cortactin (Cttn), [NM_007803]	3.2	151661814	151662852	151685467	151688252
Cutc	cutC copper transporter homolog (*E. coli*) (Cutc), [NM_025530]	2.2	43813760	43815051	43808161	43809621
Cwc15	CWC15 homolog (*S. cerevisiae*)	5.8	14337063	14338038	14359806	14363422
Cxcl12	chemokine (C-X-C motif) ligand 12 (Cxcl12), [NM_001012477]	3.5	117099526	117100316	117115608	117120445
Cyb5b	cytochrome b5 type B (Cyb5b), nuclear gene encoding mitochondrial protein [NM_025558]	70.8	109677019	109678238	109728409	109730754
Cybrd1	cytochrome b reductase 1 (Cybrd1) [NM_028593]	5.1	70983557	70984457	70981996	70984566
Cyp19a1	cytochrome P450, family 19, subfamily a, polypeptide 1 (Cyp19a1) [NM_007810]	347.4	54123560	54124297	54117520	54119036
Cyp2d22	cytochrome P450, family 2, subfamily d, polypeptide 22 (Cyp2d22), [NM_001163472]	2.4	82201202	82202492	82202769	82205394
Cyp2d34	cytochrome P450, family 2, subfamily d, polypeptide 34 (Cyp2d34) [NM_145474]	18.7	82467890	82468596	82467079	82468837
Cyp2d9	cytochrome P450, family 2, subfamily d, polypeptide 9 (Cyp2d9) [NM_010006]	5.3	82293841	82294608	82271331	82273179
Cyp4f15	cytochrome P450, family 4, subfamily f, polypeptide 15 (Cyp4f15) [NM_134127]	2.4	32812210	32813491	32812335	32813859
D030016E14Rik	RIKEN cDNA D030016E14 gene (D030016E14Rik) [NM_177240]	325.4	48602856	48603637	48590517	48591751
D10Wsu102e	DNA segment, Chr 10, Wayne State University 102, expressed (D10Wsu102e) [NM_026579]	2.9	82867774	82868986	82867602	82868637
D1Pas1	DNA segment, Chr 1, Pasteur Institute 1 (D1Pas1) [NM_033077]	2	188776272	188777281	188809717	188810850
D3Bwg0562e	DNA segment, Chr 3, Brigham & Women's Genetics 0562 expressed (D3Bwg0562e) [NM_177664]	41	117062581	117063640	117062406	117064002
D6Wsu163e	DNA segment, Chr 6, Wayne State University 163, expressed	5.8	126892081	126893185	126902043	126904143
Daam2	dishevelled associated activator of morphogenesis 2 (Daam2) [NM_001008231]	4.7	49684920	49685951	49701309	49704335
Dab1	disabled homolog 1 (*Drosophila*) (Dab1), [NM_177259]	3.5	103350573	103351235	103291416	103294850
Dact2	dapper homolog 2, antagonist of beta-catenin (*Xenopus*) (Dact2) [NM_172826]	2.2	14312879	14313924	14332072	14335590
Daglb	diacylglycerol lipase, beta	15	144255269	144255881	144247629	144251414
Dao	D-amino acid oxidase (Dao) [NM_010018]	4.3	114459657	114460264	114457662	114458898
Dcaf12l2	DDB1 and CUL4 associated factor 12–ike 2 (Dcaf12l2) [NM_175539]	4.5	41726488	41726946	41720324	41722088
Dclre1a	DNA cross-link repair 1A, PSO2 homolog (*S. cerevisiae*) (Dclre1a) [NM_018831]	2.1	56601784	56602327	56611934	56612796
Dcp1a	DCP1 decapping enzyme homolog A (*S. cerevisiae*) (Dcp1a) [NM_133761]	9.3	31220319	31221039	31166631	31168523
Ddo	D-aspartate oxidase (Ddo) [NM_027442]	58.6	40327973	40328676	40349692	40351899
Dhrs7c	dehydrogenase/reductase (SDR family) member 7C (Dhrs7c) [NM_001013013]	11.1	67629030	67630007	67627501	67629907
Dhtkd1	dehydrogenase E1 and transketolase domain containing 1	3.8	5853060	5853953	5848197	5851089
Dhx15	DEAH (Asp-Glu-Ala-His) box polypeptide 15 (Dhx15), [NM_007839]	2.7	52492375	52493572	52519619	52520751
Dio3os	deiodinase, iodothyronine type III, opposite strand (Dio3os), non-coding RNA [NR_002866]	128.5	111481076	111482560	111512540	111521526
Dirc2	disrupted in renal carcinoma 2 (human) (Dirc2) [NM_153550]	2.8	35763802	35764494	35749125	35750301
Dlk1	delta-like 1 homolog (*Drosophila*)	16.3	110697606	110698629	110690011	110699920
Dmrt2	doublesex and mab-3 related transcription factor 2 (Dmrt2) [NM_145831]	41.7	25735078	25735740	25724174	25725445
Dmrt3	doublesex and mab-3 related transcription factor 3 (Dmrt3) [NM_177360]	3.3	25712535	25713239	25689401	25690588
Dock4	dedicator of cytokinesis 4 (Dock4) [NM_172803]	11.4	41255227	41255892	41225286	41226753
Dock5	dedicator of cytokinesis 5 (Dock5) [NM_177780]	103.7	68593078	68593625	68569101	68570132

Dpf3	D4, zinc and double PHD fingers, family 3 (Dpf3) [NM_058212]	7.2	84432221	84433547	84441161	84444461
Dpysl3	dihydropyrimidinase-like 3 (Dpysl3), [NM_009468]	2.6	43613083	43613553	43596761	43598667
Dtx1	deltex 1 homolog (*Drosophila*) (Dtx1) [NM_008052]	2.3	121172131	121172947	121168645	121171409
Dusp26	dual specificity phosphatase 26 (putative) (Dusp26) [NM_025869]	9.3	32144360	32145495	32198334	32202891
Dync1i1	dynein cytoplasmic 1 intermediate chain 1 (Dync1i1), [NM_010063]	67.3	5683181	5683938	5675465	5676737
E130203B14Rik	RIKEN cDNA E130203B14 gene (E130203B14Rik) [NM_178791]	5.5	33682521	33683419	33671171	33675274
E2f6	E2F transcription factor 6 (E2f6), [NM_033270]	2.6	16828581	16829921	16831444	16832670
Ebf3	early B-cell factor 3 (Ebf3), [NM_010096]	2.8	144495309	144496028	144500235	144502964
Eepd1	endonuclease/exonuclease/phosphatase family domain containing 1 (Eepd1) [NM_026189]	5.7	25294873	25295942	25183958	25186420
Efna5	ephrin A5 (Efna5), [NM_010109]	2.4	62971932	62972586	63275746	63277334
Efnb2	ephrin B2 (Efnb2) [NM_010111]	2.1	8583574	8584431	8576063	8577627
Ehd3	EH-domain containing 3 (Ehd3) [NM_020578]	306.9	74148635	74149444	74153492	74155306
Eif2ak4	eukaryotic translation initiation factor 2 alpha kinase 4 (Eif2ak4), [NM_013719]	9.1	118233731	118234519	118233068	118234731
Eif2s2	eukaryotic translation initiation factor 2, subunit 2 (beta) (Eif2s2) [NM_026030]	5.2	154750435	154751031	154766880	154769061
Eif4g2	eukaryotic translation initiation factor 4, gamma 2 (Eif4g2), [NM_013507]	5.2	118317135	118318392	118353426	118356815
Elovl5	ELOVL family member 5, elongation of long chain fatty acids (yeast) (Elovl5) [NM_134255]	30.5	77733902	77734540	77771344	77772606
Eml4	echinoderm microtubule associated protein like 4 (Eml4), [NM_199466]	7.1	83801565	83802967	83801718	83802865
Emr1	EGF-like module containing, mucin-like, hormone receptor–like sequence 1 (Emr1) [NM_010130]	5.1	57559259	57560072	57483307	57484654
Emx2	empty spiracles homolog 2 (*Drosophila*) (Emx2) [NM_010132]	2	59610969	59611504	59541418	59547500
En2	engrailed 2 (En2) [NM_010134]	189.5	28484078	28486270	28481211	28488209
Enpep	glutamyl aminopeptidase (Enpep) [NM_007934]	18	129034175	129035102	129034285	129035969
Epb4.1l2	erythrocyte protein band 4.1-like 2 (Epb4.1l2), [NM_013511]	4.3	25053949	25054854	25154141	25155133
Epb4.1l3	erythrocyte protein band 4.1-like 3	3	69448130	69449437	69456776	69458413
Epb4.1l4a	erythrocyte protein band 4.1-like 4a (Epb4.1l4a) [NM_013512]	139.6	34132656	34133232	34145201	34148943
Esd	esterase D/formylglutathione hydrolase (Esd) [NM_016903]	11.9	75154806	75155736	75117393	75118826
Exoc6	exocyst complex component 6	7.4	37641605	37642303	37643554	37644547
Eya1	eyes absent 1 homolog (*Drosophila*) (Eya1), [NM_010164]	2.6	14358181	14358709	14269082	14270000
Eya4	eyes absent 4 homolog (*Drosophila*)	14.5	23010080	23010634	23067603	23070902
Fabp1	fatty acid–binding protein 1, liver (Fabp1) [NM_017399]	13.1	71166592	71167421	71147233	71149277
Fads2	fatty acid desaturase 2 (Fads2) [NM_019699]	2.2	10202221	10202877	10174289	10177255
Fam123a	family with sequence similarity 123, member A (Fam123a), [NM_028113]	2.5	60940404	60941073	60995935	60999444
Fam13c	family with sequence similarity 13, member C (Fam13c), [NM_024244]	2.1	69915365	69915978	69913619	69914682
Fam161b	family with sequence similarity 161, member B (Fam161b) [NM_172581]	28.2	85713821	85714727	85711867	85714774
Fam168b	family with sequence similarity 168, member B (Fam168b), [NM_174997]	2.9	34874041	34875605	34879765	34881931
Fam46c	family with sequence similarity 46, member C (Fam46c) [NM_001142952]	24.4	100273078	100273897	100275638	100277848
Fam53a	family with sequence similarity 53, member A (Fam53a) [NM_178390]	2.4	33967496	33968596	33954329	33956309
Fam76a	family with sequence similarity 76, member A (Fam76a), [NM_145553]	2.2	132467943	132469029	132459804	132461821
Far1	fatty acyl CoA reductase 1	4.4	120649689	120650486	120649807	120650730
Fat3	FAT tumor suppressor homolog 3 (*Drosophila*) (Fat3) [NM_001080814]	123.6	16122213	16122902	16128450	16129617
Fbxl17	F-box and leucine-rich repeat protein 17 (Fbxl17) [NM_015794]	6.9	63881495	63882060	63772994	63774019
Fbxl22	F-box and leucine-rich repeat protein 22 (Fbxl22) [NM_175206]	7.6	66307520	66308341	66351473	66353912
Fbxo10	F-box protein 10 (Fbxo10) [NM_001024142]	97.8	45090369	45091208	45084181	45085647
Fer1l4	fer-1–like 4 (*C. elegans*) (Fer1l4) [NM_001136556]	3.3	155862521	155863473	155867863	155875932
Fez1	fasciculation and elongation protein zeta 1 (zygin I)	2.2	36672756	36673308	36639755	36642362
Ffar2	free fatty acid receptor 2 (Ffar2), [NM_146187]	197.3	31614394	31615194	31617204	31618194
Fgf5	fibroblast growth factor 5 (Fgf5) [NM_010203]	67.3	98703007	98703809	98684254	98685884
Fgf7	fibroblast growth factor 7 (Fgf7) [NM_008008]	12.5	125800809	125801659	125854461	125855509
Fgfr2	fibroblast growth factor receptor 2 (Fgfr2), [NM_010207]	6.1	140244618	140245749	140260858	140264353
Fgg	fibrinogen gamma chain (Fgg) [NM_133862]	133.5	82816301	82817057	82798474	82800174

Fignl1	fidgetin-like 1 (Fignl1), [NM_021891]	4.5	11685597	11686692	11676316	11677899
Flt1	FMS-like tyrosine kinase 1	8.7	148441802	148443646	148536080	148539631
Fndc1	fibronectin type III domain containing 1 (Fndc1) [NM_001081416]	2.1	7963942	7965415	8017678	8021460
Fndc3c1	fibronectin type III domain containing 3C1 (Fndc3c1) [NM_001007580]	44.1	103704651	103705485	103680247	103681824
Foxc1	forkhead box C1 (Foxc1) [NM_008592]	7.6	31931485	31932573	31897160	31900990
Foxp2	forkhead box P2 (Foxp2), [NM_053242]	2.4	14781006	14781545	14847899	14852567
Fras1	Fraser syndrome 1 homolog (human) (Fras1) [NM_175473]	2.2	96776911	96777726	96867388	96869253
Frmd6	FERM domain containing 6 (Frmd6) [NM_028127]	3.5	71865200	71865693	71978532	71980073
Frmpd3	FERM and PDZ domain containing 3 (Frmpd3) [NM_177750]	2	136940795	136941515	136876324	136877842
Ftcd	formiminotransferase cyclodeaminase (Ftcd) [NM_080845]	8.7	76043682	76044823	76037615	76040120
Fth1	ferritin heavy chain 1 (Fth1) [NM_010239]	2.6	10045629	10046267	10028630	10029974
Fzd5	frizzled homolog 5 (*Drosophila*) (Fzd5), [NM_022721]	169.7	64790734	64791806	64835737	64838617
Gap43	growth associated protein 43 (Gap43) [NM_008083]	4.6	42371712	42372773	42291701	42292758
Gcap14	granule cell antiserum positive 14 (Gcap14), [NM_027045]	2.6	37799652	37800232	37787539	37788428
Gdf10	growth differentiation factor 10 (Gdf10) [NM_145741]	264.5	34727870	34728822	34735754	34739801
Ggnbp1	gametogenetin-binding protein 1	8.7	27123211	27124686	27124988	27126470
Gja8	gap junction protein, alpha 8 (Gja8) [NM_008123]	3.9	96733623	96735186	96722522	96724563
Gli3	GLI-Kruppel family member GLI3 (Gli3) [NM_008130]	3.1	15471609	15472464	15494123	15495767
Gm12824	predicted gene 12824 (Gm12824) [NM_001085549]	62.1	114149735	114151297	114077993	114080364
Gm16532	predicted gene, 16532 (Gm16532) [NM_001134752]	2.7	6376965	6378458	6367308	6368886
Gm608	predicted gene 608 (Gm608) [NM_001029889]	8	44188670	44189320	44218289	44220169
Gm9725	predicted gene 9725	3.6	83509006	83510432	83509359	83510823
Gmpr	guanosine monophosphate reductase (Gmpr) [NM_025508]	18.9	45687147	45687983	45610018	45612918
Got1	glutamate oxaloacetate transaminase 1, soluble (Got1) [NM_010324]	19.7	43578850	43580519	43578258	43580563
Got2	glutamate oxaloacetate transaminase 2, mitochondrial (Got2), nuclear gene encoding mitochondrial protein [NM_010325]	6.4	98447328	98448179	98431423	98433231
Gprc5b	G protein–coupled receptor, family C, group 5, member B (Gprc5b), [NM_022420]	6.9	126147152	126148348	126153522	126156515
Grem2	gremlin 2 homolog, cysteine knot superfamily (*Xenopus laevis*) (Grem2) [NM_011825]	3.2	176847002	176847697	176851288	176852334
Gria1	glutamate receptor, ionotropic, AMPA1 (alpha 1) (Gria1), [NM_008165]	4.2	56823863	56824708	56824380	56825801
Grik4	glutamate receptor, ionotropic, kainate 4 (Grik4) [NM_175481]	3.6	42798533	42799104	42757679	42759815
Gsdmc	gasdermin C (Gsdmc) [NM_031378]	2	63579928	63580597	63527330	63528145
Gstm4	glutathione S-transferase, mu 4 (Gstm4), [NM_026764]	4.9	107854243	107854753	107864574	107866436
Gtl3	gene trap locus 3 (Gtl3) [NM_008187]	2.8	97970049	97971667	97934524	97936098
Gucy1b3	guanylate cyclase 1, soluble, beta 3 (Gucy1b3), [NM_017469]	4.1	81868751	81869356	81877314	81879142
Gypc	glycophorin C (Gypc) [NM_001048207]	23.8	32702088	32704674	32690768	32692830
Hacl1	2-hydroxyacyl-CoA lyase 1 (Hacl1) [NM_019975]	4	32507537	32508222	32466193	32467519
Haus4	HAUS augmin-like complex, subunit 4 (Haus4) [NM_145462]	2.3	55162348	55163437	55162093	55163987
Hcfc1	host cell factor C1 (Hcfc1) [NM_008224]	3	71209501	71210509	71192416	71196314
Hdgfrp3	hepatoma-derived growth factor, related protein 3 (Hdgfrp3) [NM_013886]	17.3	89052416	89053205	89052101	89053290
Hif1an	hypoxia-inducible factor 1, alpha subunit inhibitor (Hif1an) [NM_176958]	3.8	44675593	44676812	44645343	44651562
Hmgb4	high-mobility group box 4 (Hmgb4) [NM_027036]	117.2	127927410	127929302	127927511	127929291
Hn1l	hematological and neurological expressed 1-like	6.4	25123815	25125476	25118794	25120892
Hpd	4-hydroxyphenylpyruvic acid dioxygenase (Hpd) [NM_008277]	7.2	123651473	123652482	123630110	123633222
Hs3st2	heparan sulfate (glucosamine) 3-*O*-sulfotransferase 2 (Hs3st2) [NM_001081327]	257.4	128540756	128541586	128534503	128537429
Htr4	5 hydroxytryptamine (serotonin) receptor 4 (Htr4) [NM_008313]	3.4	62544087	62544922	62482490	62485360
Htr7	5-hydroxytryptamine (serotonin) receptor 7 (Htr7) [NM_008315]	3.2	36076825	36077881	36130795	36132801
Ido2	indoleamine 2,3-dioxygenase 2 (Ido2) [NM_145949]	125.3	25671104	25672057	25655607	25658393
Igf1r	insulin-like growth factor I receptor (Igf1r) [NM_010513]	3.6	75052750	75053930	75066616	75067918
Igfbp2	insulin-like growth factor–binding protein 2 (Igfbp2) [NM_008342]	2.3	72831487	72832327	72859492	72860930
Igfbp5	insulin-like growth factor–binding protein 5 (Igfbp5) [NM_010518]	2.6	72902175	72904233	72901792	72904275

Igfbp7	insulin-like growth factor–binding protein 7 (Igfbp7), [NM_008048]	2.4	77845732	77846543	77836199	77837534
Igsf3	immunoglobulin superfamily, member 3 (Igsf3) [NM_207205]	9.2	101229171	101230573	101167051	101167990
Ikzf1	IKAROS family zinc finger 1 (Ikzf1), [NM_001025597]	2.6	11576327	11577006	11583999	11586982
Il20rb	interleukin 20 receptor beta	3.1	100321309	100322281	100347806	100351652
Inhbb	inhibin beta-B (Inhbb) [NM_008381]	6	121220753	121221963	121312397	121323426
Irx1	Iroquois related homeobox 1 (*Drosophila*) (Irx1) [NM_010573]	2.4	72008261	72008897	72137243	72138356
Itpr1	inositol 1,4,5-trisphosphate receptor 1 (Itpr1) [NM_010585]	5.6	108253257	108254218	108185448	108186597
Jakmip3	janus kinase and microtubule interacting protein 3 (Jakmip3) [NM_028708]	4.5	146147128	146148073	146130329	146134292
Jam2	junction adhesion molecule 2 (Jam2) [NM_023844]	2.4	84766817	84767863	84773436	84775983
Jazf1	JAZF zinc finger 1 (Jazf1), [NM_001168277]	4.4	53009608	53010264	53045518	53047507
Jmjd1c	jumonji domain containing 1C (Jmjd1c), [NM_001242396]	11.4	66486706	66487641	66501285	66502703
Kalrn	kalirin, RhoGEF kinase	8.2	34513770	34514770	34571523	34575143
Kank4	KN motif and ankyrin repeat domains 4 (Kank4) [NM_172872]	2.1	98478472	98479270	98481626	98484986
Kcnh1	potassium voltage-gated channel, subfamily H (eag-related), member 1 (Kcnh1), [NM_010600]	2.2	194089626	194091535	194013224	194016061
Kcnq1	potassium voltage-gated channel, subfamily Q, member 1 (Kcnq1) [NM_008434]	13.6	150345362	150346725	150290962	150299164
Kidins220	kinase D-interacting substrate 220	3.7	25623851	25624750	25625601	25628354
Kin	antigenic determinant of rec-A protein (Kin) [NM_025280]	6	10011737	10012497	10020916	10022905
Kl	klotho (Kl) [NM_013823]	2.1	151822790	151824028	151753829	151756806
Klc1	kinesin light chain 1 (Klc1), transcript variant a [NM_008450]	2.8	113011867	113013700	112999760	113003044
Klk15	Kallikrein-related peptidase 15 (Klk15) [NM_174865]	2.3	51189829	51190740	51182531	51184298
L2hgdh	L-2-hydroxyglutarate dehydrogenase (L2hgdh), nuclear gene encoding mitochondrial protein [NM_145443]	4.7	70805162	70805851	70804264	70805780
L3mbtl4	l(3)mbt-like 4 (*Drosophila*) (L3mbtl4) [NM_177278]	8.3	68565539	68566145	68622543	68624748
Lca5	Leber congenital amaurosis 5 (human) (Lca5), [NM_027448]	49.9	83287417	83288485	83336354	83338232
Ldb3	LIM domain–binding 3 (Ldb3), [NM_001039076]	12.7	35384535	35386246	35383474	35388061
Lect2	leukocyte cell–derived chemotaxin 2 (Lect2) [NM_010702]	5.8	56650581	56651621	56639930	56641278
Lepr	leptin receptor (Lepr), [NM_001122899]	3.5	101377837	101378416	101389624	101390924
Lhx4	LIM homeobox protein 4 (Lhx4) [NM_010712]	7.6	157608115	157610195	157597261	157600966
Lonrf2	LON peptidase N-terminal domain and ring finger 2	5.2	38876503	38877031	38892288	38894129
Loxhd1	lipoxygenase homology domains 1 (Loxhd1) [NM_172834]	5.7	77530826	77532200	77546059	77548079
Lpl	lipoprotein lipase (Lpl) [NM_008509]	17.4	71398421	71399176	71439715	71440816
Lrrc17	leucine rich repeat–containing 17 (Lrrc17) [NM_028977]	8.6	21037971	21039401	21052128	21053584
Lypd1	Ly6/Plaur domain containing 1 (Lypd1) [NM_145100]	10.3	127859615	127860287	127806744	127810318
Lysmd4	LysM, putative peptidoglycan-binding, domain containing 4 (Lysmd4), transcript variant B [NM_175215]	4.5	74402698	74403340	74370565	74374961
Lyz1	lysozyme 1 (Lyz1) [NM_013590]	12.9	116733084	116733732	116760805	116761840
Map2k6	mitogen-activated protein kinase kinase 6	179.2	110288160	110288852	110270122	110271403
Mapk8ip3	mitogen-activated protein kinase 8 interacting protein 3	5.3	25066190	25067007	25060535	25062764
Mbnl2	muscleblind-like 2 (Mbnl2), [NM_175341]	10	120640871	120641782	120685157	120688978
Me2	malic enzyme 2, NAD(+)-dependent, mitochondrial (Me2), nuclear gene encoding mitochondrial protein [NM_145494]	4.2	73950219	73950944	73964203	73966118
Mef2a	myocyte enhancer factor 2A	2.8	74611293	74612542	74603472	74610028
Mobp	myelin-associated oligodendrocytic basic protein (Mobp), [NM_008614]	2.4	120057913	120058888	120057823	120058204
Mpp6	membrane protein, palmitoylated 6 (MAGUK p55 subfamily member 6) (Mpp6), [NM_019939]	14.7	50122416	50123001	50077025	50078009
Mrps31	mitochondrial ribosomal protein S31 (Mrps31), nuclear gene encoding mitochondrial protein [NM_020560]	3.9	23540121	23541454	23538276	23539706
Msi2	Musashi homolog 2 (*Drosophila*) (Msi2) [NM_054043]	337.3	88518467	88519509	88535906	88539975
Mtr	5-methyltetrahydrofolate-homocysteine methyltransferase (Mtr) [NM_001081128]	2.5	12287214	12287912	12371967	12373022
Mvk	mevalonate kinase (Mvk) [NM_023556]	3.3	114944871	114945964	114913708	114918189
Myh10	myosin, heavy polypeptide 10, non-muscle (Myh10) [NM_175260]	5.2	68515894	68516922	68504473	68507421
Myh11	myosin, heavy polypeptide 11, smooth muscle	210	14256302	14257046	14247607	14249400

	(Myh11), [NM_013607]					
Myo18b	myosin XVIIIb (Myo18b) [NM_028901]	12.9	113274311	113275702	113323254	113325971
Myof	myoferlin (Myof) [NM_001099634]	5.2	38064418	38065072	37975240	37976374
Myom2	myomesin 2 (Myom2) [NM_008664]	35.3	15071342	15072508	15062075	15064089
Myoz2	myozenin 2 (Myoz2) [NM_021503]	45.3	122768849	122769657	122815157	122817559
Mypn	myopalladin (Mypn) [NM_182992]	2.9	62667818	62668290	62641843	62642874
Myt1l	myelin transcription factor 1-like (Myt1l), [NM_001093775]	5.5	30227435	30228320	30217742	30218910
N6amt1	N-6 adenine-specific DNA methyltransferase 1 (putative) (N6amt1), [NM_026366]	2	87344364	87344934	87364603	87365850
Nceh1	arylacetamide deacetylase-like 1 (Nceh1) [NM_178772]	15.3	27083360	27084812	27140041	27141112
Ndufa10	NADH dehydrogenase (ubiquinone) 1 alpha subcomplex 10 (Ndufa10), nuclear gene encoding mitochondrial protein [NM_024197]	28.3	94285435	94286312	94335874	94337883
Ndufs4	NADH dehydrogenase (ubiquinone) Fe-S protein 4 (Ndufs4), nuclear gene encoding mitochondrial protein [NM_010887]	4.3	115205499	115205968	115015936	115018014
Nefl	neurofilament, light polypeptide	114.4	68719694	68720653	68700553	68703583
Neurl1a	neuralized homolog 1A (*Drosophila*) (Neurl1a), [NM_021360]	115.6	47340955	47343697	47272707	47278058
Neurog3	neurogenin 3 (Neurog3) [NM_009719]	2.3	61597781	61598205	61598214	61601237
Nhlrc2	NHL repeat containing 2 (Nhlrc2) [NM_025811]	2.3	56669000	56670066	56668860	56670686
Nid2	nidogen 2 (Nid2) [NM_008695]	2.1	20565626	20566556	20569511	20572273
Nnt	nicotinamide nucleotide transhydrogenase (Nnt), nuclear gene encoding mitochondrial protein, [NM_008710]	2.1	120115452	120116074	119974226	119975407
Npas1	neuronal PAS domain protein 1 (Npas1) [NM_008718]	2.3	17102916	17103985	17069471	17071861
Npffr1	neuropeptide FF receptor 1 (Npffr1) [NM_001177511]	2	61042759	61044727	61060244	61061792
Nr2c1	nuclear receptor subfamily 2, group C, member 1 (Nr2c1) [NM_011629]	42	93615075	93615782	93623712	93624921
Nr5a1	nuclear receptor subfamily 5, group A, member 1	287.5	38585787	38586956	38573100	38577039
Nsg1	neuron specific gene family member 1 (Nsg1) [NM_010942]	8.5	38565633	38567183	38555105	38559587
Nt5dc3	5'-nucleotidase domain containing 3 (Nt5dc3) [NM_175331]	16.9	86257433	86258331	86258485	86259833
Ntsr2	neurotensin receptor 2 (Ntsr2) [NM_008747]	120.7	16713871	16716406	16650161	16654444
Nup133	nucleoporin 133 (Nup133) [NM_172288]	2.5	126458922	126459882	126480630	126487454
Nxph3	neurexophilin 3 (Nxph3) [NM_130858]	2.2	95398542	95399698	95363289	95367036
Olig2	oligodendrocyte transcription factor 2 (Olig2) [NM_016967]	256.5	91199887	91200861	91211585	91213042
Oxa1l	oxidase assembly 1-like (Oxa1l) [NM_026936]	3.1	55004266	55004743	54986095	54988697
Pag1	phosphoprotein associated with glycosphingolipid microdomains 1 (Pag1), transcript variant B [NM_053182]	2.1	9861135	9862347	9861115	9862364
Pah	phenylalanine hydroxylase (Pah) [NM_008777]	525.8	87050656	87051277	86975737	86976803
Papss1	3'-phosphoadenosine 5'-phosphosulfate synthase 1 (Papss1) [NM_011863]	46.1	131264547	131265482	131275038	131277082
Parp1	poly (ADP-ribose) polymerase family, member 1 (Parp1) [NM_007415]	2.3	182532915	182533856	182489678	182490796
Parp16	poly (ADP-ribose) polymerase family, member 16 (Parp16) [NM_177460]	2.5	65077527	65078382	65055959	65057346
Pax3	paired box gene 3 (Pax3), [NM_008781]	2.2	78230394	78231211	78188737	78190820
Pbx1	pre B cell leukemia homeobox 1	5.7	170284194	170285502	170229335	170230730
Pccb	propionyl Coenzyme A carboxylase, beta polypeptide (Pccb), nuclear gene encoding mitochondrial protein [NM_025835]	169	100868046	100868925	100894207	100896938
Pcmtd2	protein-L-isoaspartate (D-aspartate) O-methyltransferase domain containing 2 (Pcmtd2) [NM_153594]	7.4	181545434	181546821	181554288	181555163
Pdcd5	programmed cell death 5 (Pdcd5) [NM_019746]	2.2	36448760	36449940	36456491	36457533
Pdcl3	phosducin-like 3 (Pdcl3) [NM_026850]	4.3	39021490	39022227	39072256	39073155
Pde11a	phosphodiesterase 11A	2.2	76164292	76164979	76175485	76178330
Pdgfra	platelet derived growth factor receptor, alpha polypeptide (Pdgfra), [NM_011058]	25.4	75623771	75624630	75548357	75553471
Pdhx	pyruvate dehydrogenase complex, component X (Pdhx), nuclear gene encoding mitochondrial protein [NM_175094]	4	102862778	102863499	102891410	102892788
Pdzrn3	PDZ domain containing RING finger 3 (Pdzrn3) [NM_018884]	2.3	101324609	101325326	101310422	101312243
Peg10	paternally expressed 10 (Peg10), [NM_001040611]	2	4703908	4705549	4703703	4705820
Peg3	paternally expressed 3	15.5	6677467	6678649	6669622	6670215
Pga5	pepsinogen 5, group I (Pga5) [NM_021453]	13.3	10733698	10734592	10743178	10751732
Pgr	progesterone receptor (Pgr) [NM_008829]	2.3	8842011	8842786	8899554	8902810
Phactr3	phosphatase and actin regulator 3 (Phactr3),	49.3	177833783	177834478	177852099	177857713

	[NM_028806]					
Phf21b	PHD finger protein 21B (Phf21b), [NM_001081166]	84.6	84666055	84668729	84682658	84688580
Pik3c2g	phosphatidylinositol 3-kinase, C2 domain containing, gamma polypeptide (Pik3c2g), [NM_207683]	18.7	139566825	139567648	139669441	139670803
Pip4k2a	phosphatidylinositol-5-phosphate 4-kinase, type II, alpha (Pip4k2a) [NM_008845]	38.7	18891866	18892415	18884656	18885826
Pitx2	paired-like homeodomain transcription factor 2 (Pitx2), [NM_001042502]	31	128880209	128880726	128901178	128903879
Pknox2	Pbx/knotted 1 homeobox 2 (Pknox2), [NM_001029838]	24.2	36921846	36922522	36951310	36956483
Plcl2	phospholipase C–like 2 (Plcl2) [NM_013880]	10.6	50739579	50740357	50647198	50649781
Plekha2	pleckstrin homology domain-containing, family A (phosphoinositide binding specific) member 2 (Plekha2) [NM_031257]	2.5	26200876	26202097	26195153	26198150
Plekhf1	pleckstrin homology domain containing, family F (with FYVE domain) member 1 (Plekhf1) [NM_024413]	2.5	39031317	39032390	39003471	39005901
Plg	plasminogen (Plg) [NM_008877]	135	12556846	12557685	12575610	12577448
Pmaip1	phorbol-12-myristate-13-acetate-induced protein 1 (Pmaip1) [NM_021451]	3.3	66659490	66660132	66564817	66565842
Pmf1	polyamine-modulated factor 1 (Pmf1) [NM_025928]	3.2	88206045	88207671	88215151	88218284
Pon1	paraoxonase 1 (Pon1) [NM_011134]	1400.9	5110007	5110666	5144250	5146366
Ppa2	pyrophosphatase (inorganic) 2	5.6	132978635	132979414	132984079	132984966
Ppap2a	phosphatidic acid phosphatase type 2A (Ppap2a), [NM_008903]	2.5	113606787	113607669	113625026	113625869
Ppapdc1a	phosphatidic acid phosphatase type 2 domain containing 1A (Ppapdc1a) [NM_001080963]	2.8	136364401	136366122	136398747	136401897
Ppm1a	protein phosphatase 1A, magnesium dependent, alpha isoform (Ppm1a) [NM_008910]	2.3	73908460	73908921	73929946	73934286
Ppm1h	protein phosphatase 1H (PP2C domain containing) (Ppm1h), [NM_176919]	2.7	122161096	122162033	122216165	122217917
Ppp2r5c	protein phosphatase 2, regulatory subunit B (B56), gamma isoform (Ppp2r5c), [NM_012023]	5.5	111717397	111718609	111695847	111697422
Prdm15	PR domain containing 15 (Prdm15) [NM_144789]	3.2	98097628	98098250	98065976	98068422
Prkcq	protein kinase C, theta (Prkcq) [NM_008859]	2.9	11072294	11073133	11093493	11094542
Prox1	prospero homeobox 1	117.1	192069048	192069954	191995614	192000125
Prr18	proline rich region 18 (Prr18), [NM_178774]	2.1	8520175	8521136	8531094	8537167
Prrx2	paired related homeobox 2	3	30707710	30708812	30699093	30704729
Psmd6	proteasome (prosome, macropain) 26S subunit, non-ATPase, 6 (Psmd6) [NM_025550]	2.3	14927659	14928944	14931992	14933650
Pvalb	parvalbumin (Pvalb) [NM_013645]	21	78040416	78041912	78040353	78043272
Rab3ip	RAB3A interacting protein (Rab3ip) [NM_001003950]	6.1	116381938	116382679	116393943	116394870
Rab43	RAB43, member RAS oncogene family (Rab43), [NM_001039394]	5.3	87750310	87751893	87770094	87772468
Rap1b	RAS related protein 1b (Rap1b) [NM_024457]	2.9	117340129	117340914	117258712	117259833
Rasgef1b	RasGEF domain family, member 1B (Rasgef1b), [NM_181318]	11.7	99598648	99599693	99804041	99806482
Rassf4	Ras association (RalGDS/AF-6) domain family member 4	3.1	116633279	116634085	116622954	116625633
Rbfox1	RNA-binding protein, fox-1 homolog (*C. elegans*) 1 (Rbfox1), [NM_021477]	290.7	6861373	6862263	6348034	6349951
Rbms3	RNA-binding motif, single stranded interacting protein (Rbms3), [NM_178660]	3.8	117586506	117587301	117509630	117510430
Rcan2	regulator of calcineurin 2 (Rcan2), [NM_207649]	3	43986545	43987252	43937577	43939859
Rchy1	ring finger and CHY zinc finger domain–containing 1 (Rchy1) [NM_026557]	5.9	92320392	92320813	92199792	92200803
Rcn3	reticulocalbin 3, EF-hand calcium-binding domain (Rcn3) [NM_026555]	7.5	52350373	52351075	52341212	52344521
Rdh10	retinol dehydrogenase 10 (all-trans) (Rdh10) [NM_133832]	2.7	16136475	16137404	16167444	16168397
Ret	ret proto-oncogene (Ret), [NM_009050]	2.2	118221375	118222141	118149621	118152069
Rhbdl3	rhomboid, veinlet-like 3 (*Drosophila*) (Rhbdl3) [NM_139228]	2	80091602	80092224	80122723	80126866
Ric8b	resistance to inhibitors of cholinesterase 8 homolog B (*C. elegans*) (Ric8b), [NM_001013441]	6.3	84400715	84401682	84370425	84373553
Rin2	Ras and Rab interactor 2	2.3	145592917	145593820	145569037	145570481
Rnf157	ring finger protein 157	4.5	116267699	116268494	116272782	116275328
Rnf165	ring finger protein 165 (Rnf165) [NM_001164504]	9.2	77713258	77714189	77801618	77805301
Rnf32	ring finger protein 32 (Rnf32) [NM_021470]	13.9	29485634	29486214	29333554	29334854
Rpap3	RNA polymerase II associated protein 3 (Rpap3) [NM_028003]	2.7	97533439	97534668	97542011	97546544
Rpf1	ribosome production factor 1 homolog (*S. cerevisiae*) (Rpf1), [NM_027371]	2.3	146193413	146194874	146195607	146196914
Rps6kc1	ribosomal protein S6 kinase polypeptide 1 (Rps6kc1) [NM_178775]	45.9	192689782	192691355	192728036	192729421
Rrm1	ribonucleotide reductase M1 (Rrm1) [NM_009103]	3.5	109553660	109554451	109578998	109580097
Rwdd2a	RWD domain containing 2A (Rwdd2a),	2.3	86476580	86477203	86483967	86485385

	[NM_027100]					
Rxfp2	relaxin/insulin-like family peptide receptor 2 (Rxfp2) [NM_080468]	8.6	150808271	150809049	150831399	150834326
Rxrg	retinoid X receptor gamma (Rxrg), [NM_009107]	4.5	169521522	169522537	169527894	169530569
Sacs	sacsin	22.1	61770961	61772474	61752904	61754399
Sall4	sal-like 4 (*Drosophila*) (Sall4), transcript variant a [NM_175303]	7.1	168597976	168599032	168593361	168596448
Samd4	sterile alpha motif domain containing 4 (Samd4), [NM_001037221]	80.2	47540750	47542685	47514748	47516911
Scaf4	SR-related CTD-associated factor 4 (Scaf4) [NM_178923]	163.8	90257532	90258555	90303225	90304465
Scrn1	secernin 1 (Scrn1) [NM_027268]	124.3	54480848	54481914	54515265	54517194
Sesn3	sestrin 3 (Sesn3) [NM_030261]	2.9	14036300	14036802	14039138	14040109
Setd2	SET domain containing 2 (Setd2) [NM_001081340]	2.8	110428106	110428910	110421097	110422707
Setd3	SET domain containing 3 (Setd3) [NM_028262]	3.7	109379727	109380645	109379723	109380639
Sfrp2	secreted frizzled-related protein 2 (Sfrp2) [NM_009144]	2.9	83546186	83546894	83565426	83571568
Sgcd	sarcoglycan, delta (dystrophin-associated glycoprotein) (Sgcd) [NM_011891]	4.1	47766766	47767550	47800643	47803327
Shisa2	shisa homolog 2 (*Xenopus laevis*) (Shisa2) [NM_145463]	5.5	60236160	60237073	60243309	60247471
Shisa9	shisa homolog 9 (*Xenopus laevis*) (Shisa9), [NM_001174086]	7	12052016	12052846	11982669	11989232
Shq1	SHQ1 homolog (*S. cerevisiae*) (Shq1) [NM_181590]	3.9	100609868	100610936	100608716	100610547
Siglec5	sialic acid–binding Ig-like lectin 5 (Siglec5) [NM_145581]	3	50621866	50622457	50609751	50611451
Sirt2	sirtuin 2 (silent mating type information regulation 2, homolog) 2 (*S. cerevisiae*) (Sirt2), [NM_022432]	135.1	29543299	29545476	29540142	29548742
Slc10a7	solute carrier family 10 (sodium/bile acid cotransporter family), member 7 (Slc10a7) [NM_029736]	11.9	81060535	81061305	81096516	81099222
Slc19a3	solute carrier family 19 (sodium/hydrogen exchanger), member 3 (Slc19a3) [NM_030556]	2.8	83056503	83057360	83041309	83042570
Slc22a1	solute carrier family 22 (organic cation transporter), member 1 (Slc22a1) [NM_009202]	2.3	12848036	12849292	12877696	12882929
Slc22a3	solute carrier family 22 (organic cation transporter), member 3 (Slc22a3) [NM_011395]	2.2	12695672	12696448	12699149	12702277
Slc35f1	solute carrier family 35, member F1 (Slc35f1) [NM_178675]	3.9	52471777	52472601	52409777	52411965
Slc36a3	solute carrier family 36 (proton/amino acid symporter), member 3 (Slc36a3) [NM_172258]	2.2	54964093	54965918	54970483	54972033
Slc37a3	solute carrier family 37 (glycerol-3-phosphate transporter), member 3 (Slc37a3) [NM_028123]	5.1	39285267	39286072	39283955	39286146
Slc38a1	solute carrier family 38, member 1 (Slc38a1), [NM_134086]	51.1	96440511	96442054	96470972	96474286
Slc6a12	solute carrier family 6 (neurotransmitter transporter, betaine/GABA), member 12 (Slc6a12) [NM_133661]	32	121310087	121312397	121301439	121304278
Slc9a2	solute carrier family 9 (sodium/hydrogen exchanger), member 2	26.1	40751088	40751884	40737107	40740105
Slco2b1	solute carrier organic anion transporter family, member 2b1 (Slco2b1), [NM_175316]	7.3	106855450	106858249	106852796	106862898
Slco3a1	solute carrier organic anion transporter family, member 3a1 (Slco3a1), [NM_023908]	2.4	81684280	81684984	81651701	81653290
Slit2	slit homolog 2 (*Drosophila*) (Slit2) [NM_178804]	4	48366533	48367568	48373568	48378181
Slit3	slit homolog 3 (*Drosophila*) (Slit3) [NM_011412]	3.4	34892566	34893227	34933920	34938027
Smad1	MAD homolog 1 (*Drosophila*) (Smad1) [NM_008539]	7.2	81987486	81988513	82016385	82018522
Smtnl1	smoothelin-like 1 (Smtnl1) [NM_024230]	15.2	84662732	84663871	84661047	84663518
Smyd3	SET and MYND domain containing 3 (Smyd3) [NM_027188]	2.7	181416681	181417373	181198865	181200135
Sncaip	synuclein, alpha interacting protein (synphilin) (Sncaip), [NM_026408]	2.5	52965891	52966575	53028063	53029154
Snrnp48	small nuclear ribonucleoprotein 48 (U11/U12) (Snrnp48) [NM_026382]	8.5	38311070	38311759	38352282	38354233
Snrpa1	small nuclear ribonucleoprotein polypeptide A' (Snrpa1) [NM_021336]	24.3	73146057	73146648	73177283	73182587
Sord	sorbitol dehydrogenase (Sord) [NM_146126]	3.1	122086937	122088462	122080826	122082442
Sox7	SRY (sex determining region Y)-box 7	2.3	64575692	64577256	64566170	64568324
Spn	sialophorin (Spn), [NM_009259]	176.8	134295696	134296324	134277437	134282166
Srebf2	sterol regulatory element-binding factor 2	9.7	82000082	82001007	81970314	81972423
Srp9	signal recognition particle 9	7.8	184057482	184058385	184028287	184031102
Srpk2	serine/arginine-rich protein specific kinase 2 (Srpk2) [NM_009274]	3.3	23193594	23194284	23197396	23198313
Srrm4	serine/arginine repetitive matrix 4 (Srrm4) [NM_026886]	3.1	117030794	117032320	117040599	117044462
St3gal5	ST3 beta-galactoside alpha-2,3-sialyltransferase 5 (St3gal5), [NM_011375]	18.3	71999875	72001146	72030457	72031949
St7	suppression of tumorigenicity 7	3.5	17631194	17632402	17631278	17632316

Stbd1	starch-binding domain 1 (Stbd1) [NM_175096]	4.2	93013372	93013966	93013994	93015511
Stc2	stanniocalcin 2 (Stc2) [NM_011491]	73	31313202	31314557	31259329	31261702
Steap3	STEAP family member 3	238	122190287	122191124	122183513	122185343
Stk35	serine/threonine kinase 35 (Stk35), [NM_183262]	4.9	129685713	129686506	129654009	129657780
Stmn2	stathmin-like 2 (Stmn2) [NM_025285]	2.6	8510031	8511800	8509904	8512007
Stmn4	stathmin-like 4 (Stmn4) [NM_019675]	8.3	67032419	67033089	66962049	66964796
Stox2	storkhead box 2 (Stox2), [NM_175162]	11.8	48441583	48442320	48433051	48435200
Stx17	syntaxin 17 (Stx17) [NM_026343]	4.7	48153216	48153788	48114122	48115740
Sub1	SUB1 homolog (*S. cerevisiae*) (Sub1) [NM_011294]	2	11985035	11985867	11968636	11970295
Suclg1	succinate-CoA ligase, GDP-forming, alpha subunit (Suclg1), nuclear gene encoding mitochondrial protein [NM_019879]	10	73228996	73230031	73221259	73223123
Sulf1	sulfatase 1 (Sulf1), [NM_172294]	2.8	12808021	12808857	12825256	12826913
Sulf2	sulfatase 2 (Sulf2), [NM_028072]	2.2	165917316	165919880	165973962	165978031
Svep1	sushi, von Willebrand factor type A, EGF and pentraxin domain containing 1 (Svep1) [NM_022814]	9.4	58206952	58207823	58218052	58220273
Svil	supervillin	4	4944264	4945633	4944345	4945694
Synpo2	synaptopodin 2	138.8	122867058	122867794	122885450	122886646
Syt3	synaptotagmin III (Syt3), [NM_016663]	2.3	51625271	51626234	51605281	51617079
Tac1	tachykinin 1 (Tac1) [NM_009311]	2	7503807	7505601	7503957	7507059
Tbc1d2	TBC1 domain family, member 2 (Tbc1d2) [NM_198664]	126.4	46693161	46694221	46654111	46659735
Tbc1d21	TBC1 domain family, member 21	7.4	58198675	58199823	58226243	58227483
Tbc1d4	TBC1 domain family, member 4 (Tbc1d4) [NM_001081278]	3.3	101971461	101972283	101912381	101913466
Tbx15	T-box 15 (Tbx15) [NM_009323]	2.6	99100098	99101303	99042053	99047264
Tdrd7	tudor domain containing 7 (Tdrd7) [NM_146142]	2.8	45990976	45991755	45976944	45978797
Tlx1	T-cell leukemia, homeobox 1 (Tlx1) [NM_021901]	4.3	45208155	45208799	45214300	45223545
Tmem119	transmembrane protein 119 (Tmem119) [NM_146162]	3.7	114256923	114258622	114262610	114267333
Tmem132b	transmembrane protein 132B (Tmem132b) [NM_001190352]	241.2	126052235	126053318	126267198	126268640
Tmem132c	transmembrane protein 132C (Tmem132c) [NM_175432]	18.4	127665627	127666494	127720669	127725331
Tmem2	transmembrane protein 2 (Tmem2), [NM_031997]	2.2	21881677	21882472	21890257	21891340
Tmod1	tropomodulin 1	2.7	46036680	46037538	46051482	46057425
Tmod2	tropomodulin 2 (Tmod2), [NM_001038710]	3.3	75445942	75446695	75457886	75459846
Tnks	tankyrase, TRF1-interacting ankyrin-related ADP-ribose polymerase	23.6	36106211	36106877	36174080	36175636
Tox3	TOX high mobility group box family member 3 (Tox3) [NM_172913]	100.1	92824093	92824894	92870137	92873228
Traf3	TNF receptor-associated factor 3 (Traf3), [NM_011632]	2.3	112408784	112409386	112397726	112401303
Trak1	trafficking protein, kinesin binding 1	2.2	121198097	121199100	121200754	121205400
Trappc9	trafficking protein particle complex 9	2	72853465	72856144	72881432	72885933
Trdn	triadin (Trdn) [NM_029726]	8.1	32791136	32791832	33059512	33060737
Treml1	triggering receptor expressed on myeloid cells-like 1 (Treml1) [NM_027763]	31.6	48504602	48506848	48504585	48506412
Trerf1	transcriptional regulating factor 1 (Trerf1), [NM_172622]	7	47259860	47261139	47303358	47307707
Trib2	tribbles homolog 2 (*Drosophila*) (Trib2) [NM_144551]	5.5	15748885	15749533	15821023	15824594
Trim45	tripartite motif-containing 45 (Trim45), [NM_194343]	3.8	100687232	100688046	100731680	100732667
Trim54	tripartite motif-containing 54 (Trim54) [NM_021447]	31.9	31418882	31419870	31418522	31419723
Trim67	tripartite motif-containing 67 (Trim67) [NM_198632]	25.9	127306430	127308157	127315282	127323249
Tro	trophinin (Tro), [NM_019548]	4	147088514	147089026	147090537	147092393
Trp53inp2	transformation related protein 53 inducible nuclear protein 2 (Trp53inp2) [NM_178111]	4.5	155240600	155241406	155201450	155203740
Trpc1	transient receptor potential cation channel, subfamily C, member 1	3.2	95600582	95601311	95649515	95651198
Trpc7	transient receptor potential cation channel, subfamily C, member 7 (Trpc7) [NM_012035]	4.5	56951110	56952192	56906011	56909110
Tshz1	teashirt zinc finger family member 1 (Tshz1) [NM_001081300]	4	84246540	84247476	84220230	84222053
Tshz2	teashirt zinc finger family member 2 (Tshz2) [NM_080455]	9.8	169498981	169499691	169457535	169460201
Tshz3	teashirt zinc finger family member 3 (Tshz3) [NM_172298]	2.2	37492733	37493765	37492700	37493939
Tspan3	tetraspanin 3 (Tspan3) [NM_019793]	10.7	55989486	55990071	56038884	56041411
Tspan8	tetraspanin 8 (Tspan8), [NM_146010]	4.2	115221521	115222082	115216920	115218216
Ttc30a1	tetratricopeptide repeat domain 30A1 (Ttc30a1) [NM_030188]	2.2	75871508	75872120	75834579	75836837
Ttc32	tetratricopeptide repeat domain 32 (Ttc32) [NM_029321]	12.4	9106720	9107553	9056130	9062166
Ttc4	tetratricopeptide repeat domain 4 (Ttc4), [NM_028209]	10	106366049	106368582	106354054	106355526
Ttc7b	tetratricopeptide repeat domain 7B (Ttc7b)	4.1	101736979	101738322	101716041	101721532

	[NM_001033213]					
Ttll7	tubulin tyrosine ligase–like family, member 7 (Ttll7) [NM_027594]	198.2	146531589	146532187	146578616	146580183
Ttn	titin (Ttn), transcript variant N2-A [NM_011652]	4	76744022	76744755	76807198	76808538
Txndc5	thioredoxin domain containing 5 (Txndc5) [NM_145367]	35.5	38641619	38642258	38629125	38630624
Uggt1	UDP-glucose glycoprotein glucosyltransferase 1 (Uggt1) [NM_198899]	3.7	36225320	36226045	36309499	36313520
Uhrf1bp1	UHRF1 (ICBP90) binding protein 1 (Uhrf1bp1) [NM_001080769]	5.8	27987660	27988398	28011158	28014939
Umps	uridine monophosphate synthetase (Umps) [NM_009471]	3.2	33983532	33984301	33997189	33999783
Unc13a	unc-13 homolog A (*C. elegans*) (Unc13a) [NM_001029873]	2.1	74168143	74169168	74167888	74171172
Unc5cl	unc-5 homolog C (*C. elegans*)-like (Unc5cl) [NM_152823]	58.7	48651810	48652769	48598587	48600491
Unc79	unc-79 homolog (*C. elegans*) (Unc79) [NM_001081017]	2.6	104162021	104162789	104186398	104188535
Upb1	ureidopropionase, beta (Upb1) [NM_133995]	28.9	74837900	74838632	74868760	74870452
Use1	unconventional SNARE in the ER 1 homolog (*S. cerevisiae*) (Use1), [NM_025917]	3.9	73871114	73872627	73877141	73886026
Usp29	ubiquitin-specific peptidase 29	4.5	6880296	6881101	6870470	6872648
Usp30	ubiquitin-specific peptidase 30	2.3	114560601	114563452	114554403	114558599
Usp42	ubiquitin-specific peptidase 42 (Usp42) [NM_029749]	3.9	144444285	144445384	144475226	144479456
Utp14b	UTP14, U3 small nucleolar ribonucleoprotein, homolog B (yeast) (Utp14b), [NM_001001981]	2.1	78712488	78713419	78712558	78713452
Vat1l	vesicle amine transport protein 1 homolog-like (*T. californica*) (Vat1l) [NM_173016]	24.7	116729100	116731018	116728608	116731255
Vdac3	voltage-dependent anion channel 3 (Vdac3), [NM_011696]	4	23675708	23676755	23678215	23681120
Vldlr	very low density lipoprotein receptor (Vldlr), [NM_013703]	2.8	27215041	27216127	27312294	27313639
Vti1a	vesicle transport through interaction with t-SNAREs 1A	5.8	55408847	55409876	55416100	55417693
Wbscr17	Williams-Beuren syndrome chromosome region 17 homolog (human) (Wbscr17) [NM_145218]	4.7	131871425	131872703	131780787	131784325
Wfdc3	WAP four-disulfide core domain 3 (Wfdc3) [NM_027961]	2.5	164567002	164567866	164558960	164561160
Wisp2	WNT1 inducible signaling pathway protein 2 (Wisp2) [NM_016873]	18.4	163612515	163613513	163647668	163651653
Wnt5a	wingless-related MMTV integration site 5A (Wnt5a), [NM_009524]	4.9	29264113	29264727	29255334	29256884
Xpo7	exportin 7 (Xpo7) [NM_023045]	88	71197033	71198684	71173775	71178601
Xrcc6bp1	XRCC6-binding protein 1 (Xrcc6bp1), [NM_001159559]	4.3	126335254	126336170	126326079	126328066
Zbp1	Z-DNA–binding protein 1 (Zbp1), [NM_021394]	118.6	173041305	173043285	173041109	173045625
Zeb2	zinc finger E-box–binding homeobox 2 (Zeb2), [NM_015753]	204.2	45053779	45054366	44970656	44973294
Zfp2	zinc finger protein 2 (Zfp2), [NM_001044697]	13.6	50723506	50724487	50719465	50720284
Zfp238	zinc finger protein 238 (Zfp238), [NM_013915]	3.6	179392853	179394131	179386281	179387524
Zfp369	zinc finger protein 369 (Zfp369) [NM_178364]	3.5	65411046	65411799	65410953	65412030
Zfp383	zinc finger protein 383 (Zfp383) [NM_001243908]	2.4	30660328	30661118	30648892	30651109
Zfp518b	zinc finger protein 518B (Zfp518b), [NM_001081144]	10.8	39060488	39060964	39064339	39066045
Zfp521	zinc finger protein 521 (Zfp521) [NM_145492]	10.7	14075720	14076433	14127886	14130415
Zfp607	zinc finger protein 607 (Zfp607) [NM_001024726]	4	28661198	28661989	28655938	28657550
Zfp92	zinc finger protein 92 (Zfp92) [NM_009566]	2.6	70666932	70668380	70666768	70668613
Zfr	zinc finger RNA-binding protein (Zfr) [NM_011767]	5.3	12065977	12066576	12004279	12005874
0610011L14Rik	RIKEN cDNA 0610011L14 gene (0610011L14Rik), [NM_026661]	28.5	156383285	156384943	156366470	156369464
0610040J01Rik	RIKEN cDNA 0610040J01 gene (0610040J01Rik) [NM_029554]	508	64159275	64160226	64202895	64204576
1110004F10Rik	RIKEN cDNA 1110004F10 gene (1110004F10Rik) [NM_019772]	172.2	123290936	123292664	123262748	123264502
1110032A03Rik	RIKEN cDNA 1110032A03 gene	6.8	50600617	50601198	50610935	50612362
1110038F14Rik	RIKEN cDNA 1110038F14 gene (1110038F14Rik) [NM_054099]	2.1	76765559	76766318	76762933	76766429
1300010F03Rik	RIKEN cDNA 1300010F03 gene (1300010F03Rik), [NM_173758]	8.9	79324915	79325579	79432547	79433615
1700001L19Rik	RIKEN cDNA 1700001L19 gene (1700001L19Rik) [NM_027035]	99.6	68753198	68753801	68751127	68752127
1700008A04Rik	RIKEN cDNA 1700008A04 gene (1700008A04Rik) [NM_027050]	2.4	32710972	32711814	32732218	32733874
1700011L22Rik	RIKEN cDNA 1700011L22 gene (1700011L22Rik) [NM_026315]	3	81739495	81739976	81711757	81714862
1700056E22Rik	RIKEN cDNA 1700056E22 gene (1700056E22Rik)	3.2	185926501	185926968	186017045	186018960

	[NM_028516]					
2310046A06Rik	RIKEN cDNA 2310046A06 gene (2310046A06Rik) [NM_027150]	137.1	77204923	77205753	77232795	77234161
2410076I21Rik	RIKEN cDNA 2410076I21 gene (2410076I21Rik) [NM_028598]	14.4	58600384	58601025	58600080	58601330
2700060E02Rik	RIKEN cDNA 2700060E02 gene (2700060E02Rik) [NM_026528]	3.2	20709016	20709954	20615795	20617035
4930403N07Rik	RIKEN cDNA 4930403N07 gene (4930403N07Rik) [NM_028687]	2.8	73261933	73262571	73298819	73299961
6720456H20Rik	RIKEN cDNA 6720456H20 gene (6720456H20Rik) [NM_172600]	22.2	49157918	49158600	49047830	49049540
9530059O14Rik	RIKEN cDNA 9530059O14 gene	2.1	122490155	122490785	122477125	122482835
9930013L23Rik	RIKEN cDNA 9930013L23 gene (9930013L23Rik) [NM_030728]	2.5	91247980	91248809	91233194	91237271
A530098C11Rik	RIKEN cDNA A530098C11 gene (A530098C11Rik) [NM_001013799]	13.4	44091624	44092993	44091544	44092592
A730011L01Rik	RIKEN cDNA A730011L01 gene (A730011L01Rik), [NM_177394]	4.5	119340744	119341974	119322649	119324480
A830080D01Rik	RIKEN cDNA A830080D01 gene (A830080D01Rik) [NM_001033472]	2.5	155946220	155946946	155964071	155966209
A930033H14Rik	RIKEN cDNA A930033H14 gene (A930033H14Rik), partial miscRNA [XR_105403]	2.2	68711154	68711952	68698878	68700651

Genes up-regulated in Cbx4KO cells and showing Cbx4 and H3K27me3 binding. Directly overlapping Cbx4 and H3K27me3 ChIP-seq peaks are shown in red.

Mardaryev et al., http://www.jcb.org/cgi/content/full/jcb.201506065/DC1

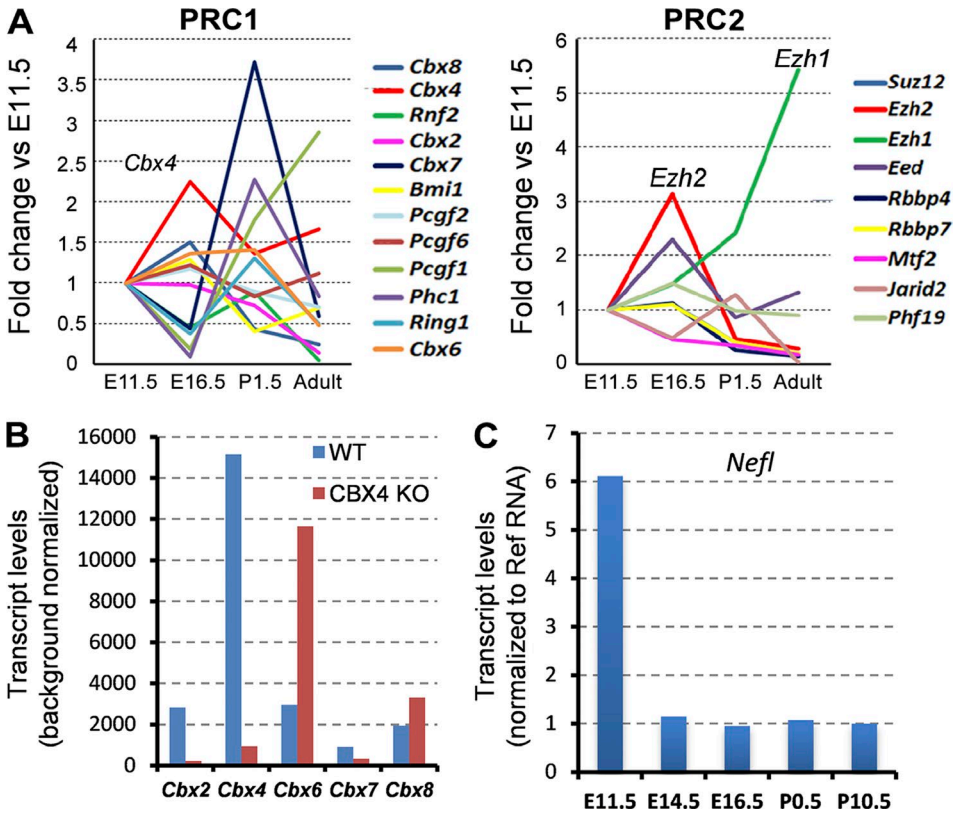

Figure S1. **Expression of the PRC1/PRC2 genes and *Nefl* gene in mouse epidermis during development.** (A) Expression of the distinct PRC1 and PRC2 genes in the laser-captured mouse epidermis during distinct stages of development (Agilent microarray values normalized to the reference RNA levels are shown relative to the corresponding expression levels in E11.5 epidermis). The data shown are from a single experiment performed in duplicate. (B) Expression of different Cbx genes in the epidermis of E16.5 WT and *Cbx4*KO mice (Agilent microarray, background-normalized data). The data shown are from a single experiment performed in duplicate (mean ± SD). $n = 2$; two-way t test. (C) Expression of the *Nefl* transcripts in WT mouse epidermis at distinct stages of development (Agilent microarray values normalized to the reference RNA levels). The data shown are from a single experiment performed in duplicate (mean ± SD; $n = 2$; one-way ANOVA).

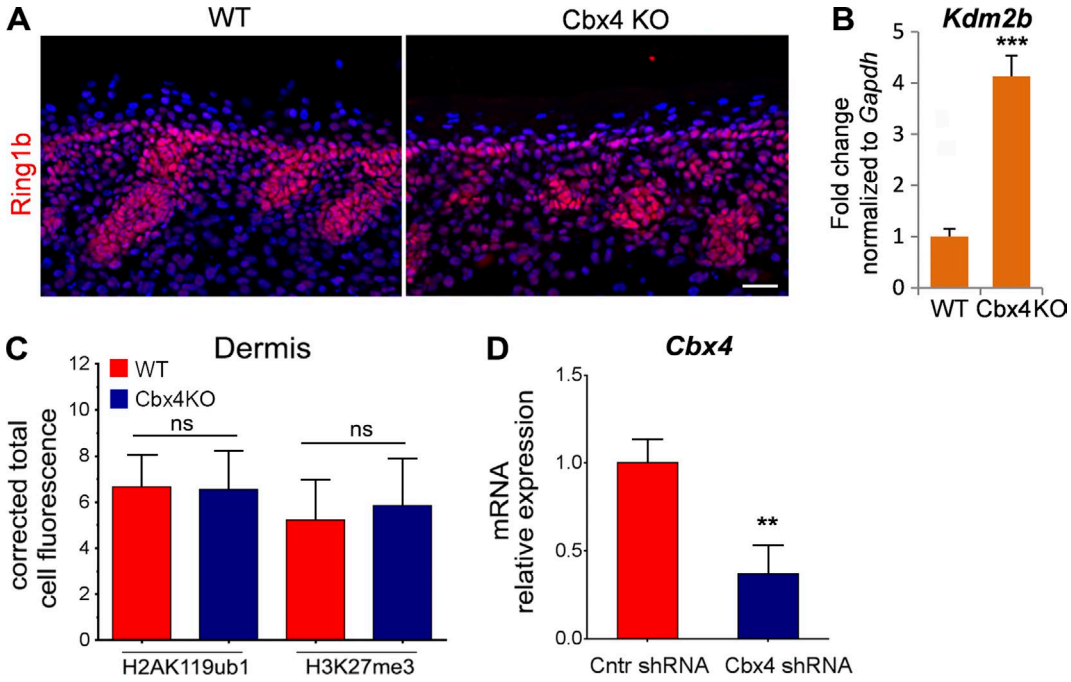

Figure S2. **Characterization of the changes in gene expression in the epidermis of Cbx4KO mice and in primary KCs after *Cbx4* knockdown.** (A) Immunofluorescence detection of Ring1b shows similar patterns of expression in the epidermis of E16.5 WT and *Cbx4*KO mice. Bar, 25 µm. (B) Kdm2b transcript levels are significantly up-regulated in the E16.5 epidermis of *Cbx4*KO mice compared with WT controls (mean ± SD; $n = 3$). (C) Correlated total cell fluorescence level of H2AK119ub1 and H3K27me3 show a lack of differences in their expression between the dermal cells of E16.5 WT and *Cbx4*KO mice. (D) Down-regulation of the *Cbx4* transcripts in the primary mouse KCs after treatment with *Cbx4* shRNA (mean ± SD; $n = 3$). **, $P < 0.01$; ***, $P < 0.001$. ns, not significant.

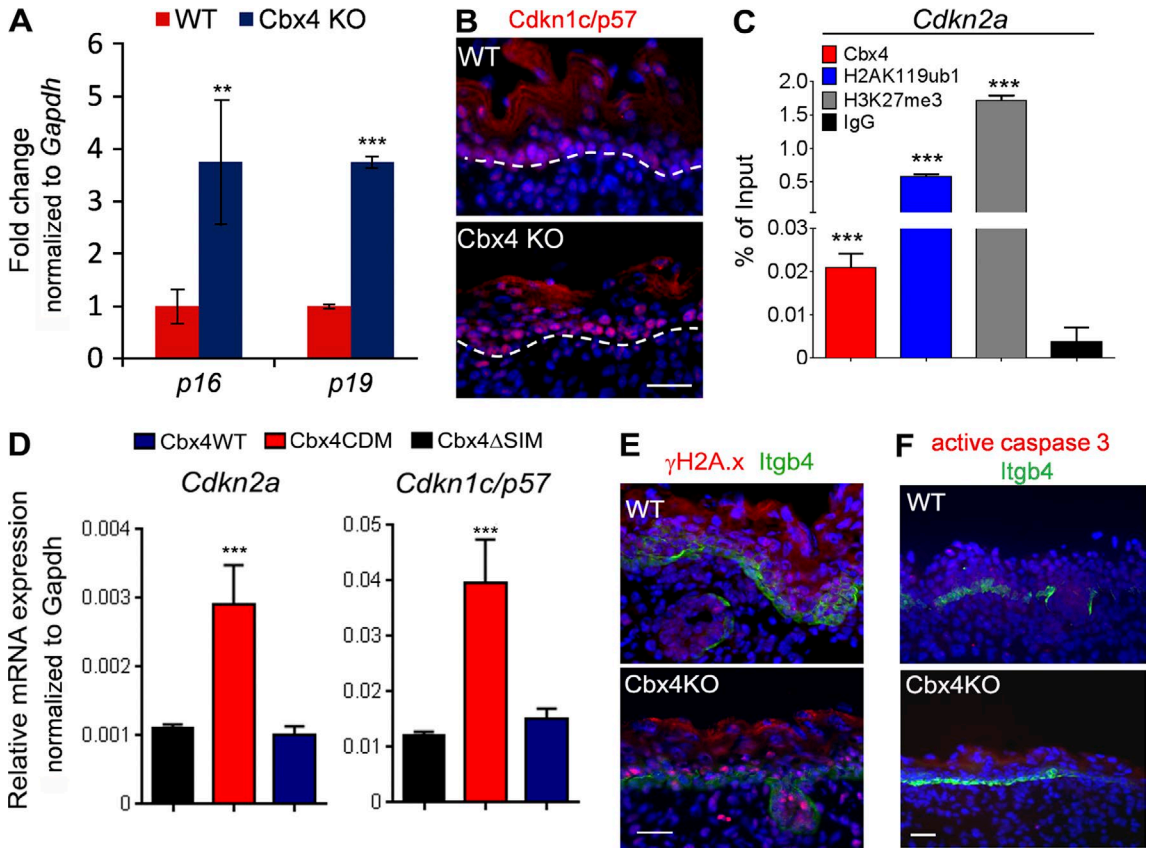

Figure S3. **Analyses of the senescence and apoptotic markers in WT and *Cbx4*-deficient skin.** (A) p16 and p19 transcript levels are significantly up-regulated in the epidermis of E16.5 *Cbx4*KO mice compared with WT controls (mean ± SD; *n* = 3). (B) Increased Cdkn1c/p57 protein expression in the epidermis of E16.5 *Cbx4*KO mice. Dashed lines separate epidermis and dermis. (C) ChIP-qPCR analyses show an enrichment for Cbx4, H2AK119ub1, and H3K27me3 in the promoter region of the *Cdkn2a* gene in primary KCs (mean ± SD; *n* = 3). (D) Increase of the levels of the *Cdkn2a* and *Cdkn1c* transcripts in primary mouse KCs infected with retrovirus expressing a mutant *Cbx4* chromodomain (*Cbx4*CDM; mean ± SD; *n* = 3). (E) Appearance of γ-H2AX–positive cells in the epidermis of E16.5 *Cbx4*KO mice. Integrin-β4 (Itgb4) expression outlines the basement membrane of the epidermis. DAPI counterstain (blue) shows the nuclei. (F) A lack of caspase 3–positive cells in the epidermis of E16.5 WT and *Cbx4*KO mice. Integrin-β4 expression outlines the basement membrane of the epidermis. DAPI counterstain (blue) shows the nuclei. Bars, 50 μm. **, P < 0.01; ***, P < 0.001.

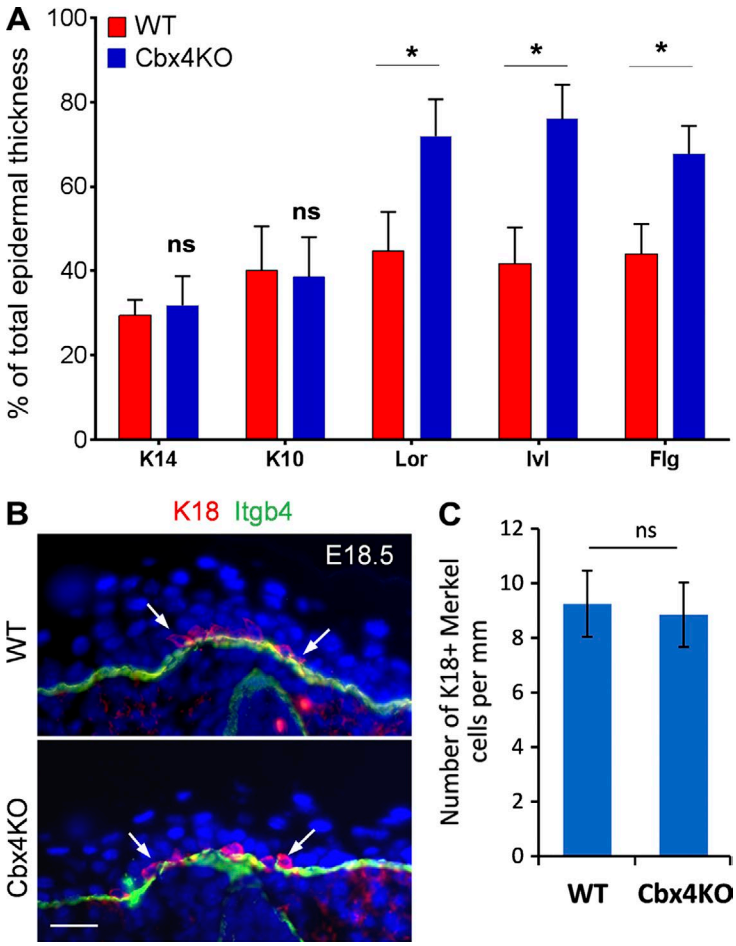

Figure S4. **The analyses of epidermal and Merkel cell differentiation in Cbx4KO and WT mice.** (A) Quantification of the ratios between different cellular layers expressing distinct markers of epidermal differentiation shows a significant increase of the cellular layers expressing the markers of terminal KC differentiation (Loricrin, Involucrin, and Filaggrin) in the epidermis of E16.5 Cbx4KO mice versus WT controls ($P < 0.01$). (B and C) Immunofluorescence analyses of the Merkel cells expressing K18 (B, arrows) show a lack of differences between the epidermis of E16.5 *Cbx4*KO and WT mice. Integrin-β4 (Itgb4) expression outlines the basement membrane of the epidermis (C). DAPI counterstain (blue) shows the nuclei. Bar, 50 µm. *, $P < 0.05$. ns, not significant.

Table S1. **Expression of PRC1 and PRC2 genes in epidermal progenitor cells at different stages of epidermal development**

Gene	E11.5		E16.5		P1.5		P56	
	Absolute values	Normalized values	Absolute values	Normalized values	Absolute values	Normalized values	Absolute values	Normalized values
PRC1								
Bmi1	4,939	0.78	890	1.00	1,959	0.32	164.19	0.54
Cbx2	10,576	2.69	2,616	2.64	7,870	1.96	1,062.61	0.40
Cbx4	5,757	0.44	5,378	0.99	8,019	0.60	7,709.26	0.74
Cbx6	26,436	1.18	4,686	1.61	39,345	1.67	196.33	0.57
Cbx7	2,643	1.00	28	0.44	12,494	3.73	369.93	0.60
Cbx8	3,995	2.38	2,623	3.58	1,548	1.03	21,910.41	0.59
Pcgf1	3,271	1.27	114	0.24	4,264	2.26	7,096.51	3.64
Pcgf2	387	1.02	22	1.21	384	0.92	230.91	0.72
Pcgf6	1,816	0.58	354	0.71	1,662	0.49	1,946.37	0.65
Phc1	29,160	1.75	135	0.17	68,436	3.99	10,662.08	1.47
Phf19	1,053	0.56	196	0.83	1,198	0.55	788.60	0.51
Ring1	1,179	1.16	69	0.44	1,831	1.51	728.27	0.59
Rnf2	1,006	0.53	28	0.24	945	0.48	181.02	0.03
Rybp	222	0.53	134	1.27	208	0.50	221.50	0.56
PRC2								
Eed	2,095	0.51	91	1.17	1,960	0.44	3,339	0.67
Ezh1	749	1.45	122	2.13	1,672	3.49	3,882	7.89
Ezh2	2,341	0.43	484	1.36	1,098	0.20	671	0.12
Jarid2	8,854	4.31	4,561	2.08	11,294	5.55	304	0.18
Mtf2	6,840	4.10	3,727	1.34	2,968	1.70	1,582	0.71
Mtf2	17,216	3.74	885	1.72	6,605	1.26	2,960	0.67
Rbbp4	28,626	2.36	10,711	2.67	6,897	0.62	4,209	0.34
Rbbp7	36,889	0.59	5,890	0.65	15,775	0.24	9,247	0.12
Suz12	14,478	0.82	2,603	0.92	4,917	0.33	1,909	0.12

Agilent Technologies whole genome microarray values: absolute expression levels (a.u.) and normalized to reference RNA.

Table S2. **Cbx4 target genes up-regulated in p63KO epidermal progenitor cells**

Gene name	p63 versus WT
0610040J01Rik	2.12
1700056E22Rik	3.42
Acot12	3.04
Atp1a2	2.13
BC051665	7.15
C8b	4.38
Cbr4	2.4
Cfi	2.01
Chmp2b	7.78
Ckmt2	2.33
Clybl	5.01
Cpn2	6.31
Ctdp1	16.58
Cyp4f15	2.21
Daglb	12.98
Dmrt2	95.42
Dmrt3	5.63
Dpysl3	3.11
Dtx1	2.26
Dusp26	4.37
Ehd3	3.13
Elovl5	2.47
Eml4	5.7
Enpep	50.8
Fer1l4	2.62
Fez1	3.97
Fndc3c1	16.5
Foxp2	2.16
Grem2	28.43
Hpd	3.47
Kcnq1	2.99
L2hgdh	2.52
Lect2	8.96
Lpl	2
Lrrc17	3.18
Lypd1	3.03
Mrps31	2.02
Nefl	23.26
Nsg1	3.67
Pah	114.77
Parp16	4.35
Pcmtd2	3.3
Pdzrn3	2.35
Pon1	20.73
Psmd6	2.34
Rasgef1b	3.04
Rpap3	3.04
Rwdd2a	5.57
Rxrg	2.97
Sfrp2	3.34
Shisa2	6.53
Slc37a3	7.02
Slc6a12	3.06
Slc9a2	56.62
Slco2b1	3.16
Sord	4.33
Sox7	21.69
Stc2	25.25
Stmn4	4.39
Sulf1	5.77
Sulf2	2.56

Table S2. **Cbx4 target genes up-regulated in p63KO epidermal progenitor cells** *(Continued)*

Gene name	p63 versus WT
Tdrd7	2.82
Tmem132c	8.1
Traf3	3.54
Tshz3	88.53
Tspan12	10.11
Unc5cl	2.71
Upb1	2.16
Utp14b	4.64
Zbp1	135.35
Zfp518b	5.81
Zfp521	6.49
0610040J01Rik	10.01
1700056E22Rik	5.85

Table S3. **Primers used for qRT-PCR analyses**

Gene	Oligos 5′- to -3′
qRT-PCR primers	
Cbx4	AGTGGAGTATCTGGTGAAATGGA
	TCCTGCCTTTCCCTGTTCTG
Cdkn2a/p16	ATGGGTCGCAGGTTCTTGGT
	ATCATCACCTGGTCCAGGATTCC
Cdkn2d/p19	CCTTGCAGGTCATGATGTTTGG
	CCAGGGCATTGACATCAGCA
En2	CTTCTTCAGGTCCCAGGT
	CAAATCTTGATCTGAGACTCGT
Flg	GAAGGAACTTCTGGAAGGACAAC
	TCCATCAGTTCCACCATGCCTC
Gapdh	GTGTTCCTACCCCCAATGTG
	AGGAGACAACCTGGTCCTCA
Ivl	GCAGGAGAAGTAGATAGAG
	TTAAGGAAGTGTGGATGG
Lhx4	CCGATGCAACAGATTCCC
	GAAGCATCTGTCAGCCAG
Kdm2b	GATGCTGAGCGGTATCATCCG
	GAGACAGCGATCCATGAGCAG
Mobp	CCAGGCTCTCCAAGAACCAG
	GGTCCACGATCTCACGCTT
Nefl	CGCCATGCAGGACACAATCA
	GAGTAGCCGCTGGTTATGCT
Neurog3	TCGTCTTTACTGCCCGCTAC
	CTAGGGCTTTCCGGTTCACA
Olig2	TCCCCAGAACCCGATGATCTT
	CGTGGACGAGGACACAGTC
Zeb2	ATTGCACATCAGACTTTGAGGAA
	ATAATGGCCGTGTCGCTTCG
Cloning primers	
Cbx4 enhancer	AATCGATAAGGATCCTTTGAGAACAGAACAAGGGT
	AGGGCATCGGTCGACGGATTTCAGACAGCCAAGG
ChIP primers	
Cbx4	TGTGTCAAAGAGACTAAGGACAGC
	AGCTCCAGTGCTCAGTGGTC
Lor	ACCAGCTTACCACTCTCCCA
	GTCTGGTCTCTCCAGTTGGC
Nefl	GTCAGAGTCCCGGCGTATAA
	AGCCGAACGAACTCATGGTG
Cdkn2a	TCGCTCCGGTTAACTTTCGG
	GCCTCGCCGATCTTCCTATT

Table S4. **List of antibodies used in this study**

Antigen	Application	Host	Dilution	Catalog number	Supplier
Caspase 3 active	IF	Rabbit	1:200	ab13847	Abcam
Cbx4	ChIP	Rabbit	5 µg	A302-355A	Bethyl Laboratories, Inc.
Cbx4	IF	Rabbit	1:100		This study/polyclonal antibody against amino acids 363–551
CD104 (Itgb4)	IF	Rat	1:100	553745	BD
Cdkn1c	IF	Rabbit	1:100	ab4058	Abcam
Filaggrin	IF	Rabbit	1:100	sc-30230	Santa Cruz Biotechnology, Inc.
gH2A.x	IF	Rabbit	1:100	39117	Active Motif
H2AK119ub1	IF/ChIP	Rabbit	1:200	8240s	Cell Signaling Technology
H3K27me3	IF/ChIP	Rabbit	1:100; 5 µg	39157	Active Motif
Involucrin	IF	Rabbit	1:100	ab53112	Abcam
Ki67	IF	Rabbit	1:100	ab15580	Abcam
Krt10	IF	Rabbit	1:100	ab76318	Abcam
Krt14	IF	Rabbit	1:100	ab7800	Abcam
Krt18	IF	Rabbit	1:100	sc-31700	Santa Cruz Biotechnology, Inc.
Loricrin	IF	Rabbit	1:1,000	PRB-145P	Covance
Nefl	IF	Rabbit	0.111111	NB300-131	Novus Biologicals
Ring1b	IF	Rabbit	1:100	5694P	Cell Signaling Technology

IF, immunofluorescence.

Table S5 is supplied as a PDF and it shows Cbx4 target genes in epidermal KCs.